Development of a design methodology for hydraulic pipelines carrying rectangular capsules.

ASIM, T., MISHRA, R., ABUSHAALA, S. and JAIN, A.

2016

DEVELOPMENT OF A DESIGN METHODOLOGY FOR HYDRAULIC PIPELINES CARRYING RECTANGULAR CAPSULES

Taimoor Asim[*1], Rakesh Mishra[2], Sufyan Abushaala[3] and Anuj Jain[4]
[1,2,3] School of Computing & Engineering
University of Huddersfield, Queensgate, Huddersfield HD1 3DH, UK
[4] Department of Applied Mechanics
Motilal Nehru National Institute of Technology, Allahabad, India
[1]t.asim@hud.ac.uk, [2]r.mishra@hud.ac.uk, [3]sufyan.abushaala@hud.ac.uk,
[4]anujjain@mnnit.ac.in

Abstract
The scarcity of fossil fuels is affecting the efficiency of established modes of cargo transport within the transportation industry. Efforts have been made to develop innovative modes of transport that can be adopted for economic and environmental friendly operating systems. Solid material, for instance, can be packed in rectangular containers (commonly known as capsules), which can then be transported in different concentrations very effectively using the fluid energy in pipelines. For economical and efficient design of such systems, both the local flow characteristics and the global performance parameters need to be carefully investigated. Published literature is severely limited in establishing the effects of local flow features on system characteristics of Hydraulic Capsule Pipelines (HCPs). The present study focuses on using a well validated Computational Fluid Dynamics (CFD) tool to numerically simulate the solid-liquid mixture flow in both on-shore and off-shore HCPs applications including bends. Discrete Phase Modelling (DPM) has been employed to calculate the velocity of the rectangular capsules. Numerical predictions have been used to develop novel semi-empirical prediction models for pressure drop in HCPs, which have then been embedded into a robust and user-friendly pipeline optimisation methodology based on Least-Cost Principle.

Keywords: *Computational Fluid Dynamics (CFD), Hydraulic Capsule Pipeline (HCP), Discrete Phase Modelling (DPM), Least-Cost Principle*

1. Introduction
Pipelines transporting capsules are becoming popular amongst cargo and transportation industries throughout the world. The capsules are hollow containers filled with different materials such as minerals, ores etc. In some cases, the material that needs to be transported can be shaped as the capsule itself. The shape of the capsules can be spherical, cylindrical or rectangular with different design considerations depending on the required application.
Primarily, there are two different types of pipelines i.e. on-shore and off-shore. On-shore pipelines mostly involve horizontal pipes, while off-shore pipelines comprise primarily of vertical pipes. Furthermore, pipe fittings, such as pipe bends etc., are an integral part of any piping system. For an effective capsule system design, interdependence of a large number of geometrical and flow and fluid related variables needs to be established, and this information unfortunately is not explicitly available in the literature, especially for pipelines transporting rectangular capsules. These systems are currently under active investigation for application into shipping industry for loading-unloading operations. In order to develop knowledge base covering a wide range of operating conditions for the analysis of HCPs, both horizontal and vertical pipelines, transporting rectangular capsules, have been considered for numerical

[*] Corresponding Author
Tel.: +44 1484 472323

analysis, supported by experimental investigations, in the present study. A variety of different pipe bends transporting capsules have also been investigated, for the sake of developing accurate design methodology. After carrying out detailed numerical analysis at component-level, a system-level optimisation study has been carried out in order to optimally design HCPs based on Least-Cost Principle. In the following sections a review of important research works carried out regarding various components of a capsule pipeline system is presented.

1.1 Hydraulic Capsule Pipelines

Hydraulic capsule pipelines have been subject of intense research activities in recent decades. The first notable investigative study in this area however started in the early 1960s when Charles [1] analysed the flow of a single cylindrical capsule of density equal to that of its carrier fluid (water). Charles developed analytical expressions for both the capsule velocity and the pressure drop in the pipeline as a function of the capsule-to-pipe hydraulic diameter ratio (k) only. However, the study lacked detailed analysis on the effects of the capsule geometry and other flow parameters on the capsule velocity and the pressure drop within the pipeline. Later, Ellis [2], Newton et al [3], Ellis et al [4] and Jan et al [5] carried out a wide range of experimental investigations on a single spherical and cylindrical capsules, for a wide range of operating conditions, and developed empirical equations for the prediction of capsule-to-flow velocity ratio as a function of non-dimensional parameters. Since mid-1970s, researchers started combining analytical studies with experimental work on hydraulic pipelines, carrying a train of capsules. Tomita et al [6-7] conducted a series of analytical studies on the flow of cylindrical capsules, focusing only on the velocity and the trajectory of the capsules, in a hydraulic pipeline. However, the capsules have been considered as point masses, and a limited discussion on the flow velocity and pressure distribution in the vicinity of the capsules has been reported. Lenau et al [8] however extended Tomita et al [6] work and developed a numerical model in which a single cylindrical capsule has been considered as both elastic and a rigid body respectively. The capsule velocity and trajectory has been found out at node points, but a very limited discussion on the pressure and velocity distributions has been presented.

Numerical analysis in the area of HCPs has first been reported by Khalil et al [9] who simulated the flow of a single cylindrical capsule in a pipeline. A comparison of various turbulence models has been presented for the velocity profiles and pressure drop calculations. Further studies were carried out by Ellis et al [10], Kruyer et al [11] and Kroonenberg [12], all regarding the flow of cylindrical capsules in HCPs. The first study that considered the flow of rectangular capsules in HCPs was carried out by Agarwal et al [13] who developed empirical relations of the velocity ratio of heavy-density capsules of various shapes. The experimental study mainly focused on measuring the capsule velocity, and hence lacks in describing the flow and capsule behaviour in HCPs. The capsule velocity data has been used in the present study as the boundary conditions of heavy density rectangular capsules in a horizontal HCP. Chow [14], Hwang et al [15], Latto et al [16] and Motoyoshi [17] all carried out experiments based parametric investigations on capsule velocities in vertical and inclined pipelines, where the shape of the capsules was always either spherical or cylindrical. These studies are in-line with most of the previous studies i.e. measurement of capsule velocity and developing empirical models for the velocity ratio. Ulusarslan et al [18-22], Vlasak et al [23-24] and Mishra [25] however started measuring the pressure drop within pipes and bends transporting spherical or cylindrical capsules/particles. However, rectangular capsules were not part of their parametric investigations. It was not until Asim et al [26-28] carried out detailed numerical analysis on the flow behaviour within hydraulic pipes and bends carrying spherical and cylindrical capsules. However, the rectangular capsules were not considered for analysis. Asim did develop semi-empirical prediction models for the determination of

capsule's friction factors and loss coefficients, and used them to develop an optimisation methodology, which is based on least cost principle. Many other researchers like Polderman [29] Morteza et al [30] and Yongbai [31] also developed optimisation methodologies; however these methodologies were mostly for granular flow pipelines. Swamee et al [32-33] developed an optimisation methodology for HCPs based on least cost principle; however, it considers the friction factor of the capsules as an input, strictly limiting the usefulness of the developed methodology. At system-level optimisation of HCPs, only limited works are available which cover a wide range of operating conditions. Hence, this study presents a modified version of Asim's [26-28] optimisation model, where rectangular capsules have been considered within the HCPs, covering a wide range of operating conditions.

2. Pressure drop considerations in HCPs

The pressure drop in a pipeline is computed using Darcy-Weisbach equation [34]:

$$\Delta P = \lambda \frac{L_p}{D} \frac{1}{2} \rho U^2 \tag{1}$$

where ΔP is the pressure drop across the pipe, λ is Darcy's friction factor, L_p is the length of the pipe, D is the diameter of the pipe, ρ is the density of fluid and U is the flow velocity within the pipe. Darcy's equation can be further used to compute pressure drop within hydraulic capsule pipelines by separating the pressure drop due to water alone, and pressure drop due to capsules only. This can be mathematically expressed as:

$$\Delta P_m = a_1 \lambda_w \frac{L_p}{D} \frac{a_2 \rho_w (1-c) a_3 U_{av}^2}{2} + a_4 \lambda_c \frac{L_p}{D} \frac{a_5 \rho_w c\, a_6 U_{av}^2}{2} \tag{2}$$

where ΔP_m represents the presser drop across the HCP, ρ_w is the density of water, c is the concentration of the solid phase (i.e. capsules), U_{av} is the average flow velocity and the constants a_1, a_2, a_3, a_4, a_5, a_6 are the coefficients which relate the friction factor, density and the velocity of both the water and the capsules respectively to that of the mixture flow. If the effects of the concentration of the solid phase c, and the constants a_1, a_2, a_3, a_4, a_5, a_6 are represented in friction factor due to water (λ_w) and friction factor due to capsules (λ_c) as:

$$\lambda_w = f(c, a_1, a_2, a_3) \tag{3}$$

$$\lambda_c = f(c, a_4, a_5, a_6) \tag{4}$$

then equation (2) can be simplified as:

$$\Delta P_m = \lambda_w \frac{L_p}{D} \frac{\rho_w U_{av}^2}{2} + \lambda_c \frac{L_p}{D} \frac{\rho_w U_{av}^2}{2} \tag{5}$$

Equation (5) is valid for horizontal HCPs. The elevation effects can also be included (for vertical HCPs) as follows:

$$\Delta P_m = \lambda_w \frac{L_p}{D} \frac{\rho_w U_{av}^2}{2} + \lambda_c \frac{L_p}{D} \frac{\rho_w U_{av}^2}{2} + \rho_w g \Delta z_w \tag{6}$$

where g is the gravitational acceleration and Δz_w is the elevation of the water column. Hence, equations (5) and (6) represent the major losses in HCPs. Similarly, minor losses within HCPs can be derived as follows:

$$\Omega = \frac{\Delta P}{\frac{1}{2}\rho U^2} \tag{7}$$

$$\Delta P_m = \Omega_w \frac{n\,\rho_w\,{U_{av}}^2}{2} + \Omega_c \frac{n\,\rho_w\,{U_{av}}^2}{2} \tag{8}$$

$$\Delta P_m = \Omega_w \frac{n\,\rho_w\,{U_{av}}^2}{2} + \Omega_c \frac{n\,\rho_w\,{U_{av}}^2}{2} + \rho_w g \Delta z_w \tag{9}$$

where Ω_w represent the loss coefficient of the bend due to water, Ω_c is the loss coefficient of the bend due to capsule and n is the number of bends attached to the pipeline. Hence, equations (8) and (9) include the minor losses within HCPs. λ_w and λ_c in equations (3) and (4) can be determined using either experimental or well verified numerical methods, where numerical methods can further provide useful information regarding the flow structure within HCPs rapidly. In the present study, these coefficients have been computed using advanced CFD based techniques. The next section provides detailed information regarding the CFD setup that has been used in the present study for the analysis of HCPs transporting cylindrical capsules.

3. Geometrical Configurations of the HCP

The geometry of the hydraulic capsule pipeline has been created using a commercial CFD package. The numerical model constitutes a 5m long inlet pipe, a 1m long test section and a 1m long outlet pipe, as shown in figure 1. A long inlet pipe has been used to accommodate the entrance length effects [35], whereas the outlet pipe fulfils solver's requirement for the boundaries of the flow domain to be far away from the area of interest, which is the test section in the present case. The HCP test section is similar to that of Ulusarslan et al [36] having an internal diameter of 0.1m. The pipe surface has been considered to be hydrodynamically smooth, with an absolute roughness constant (ε) of zero.

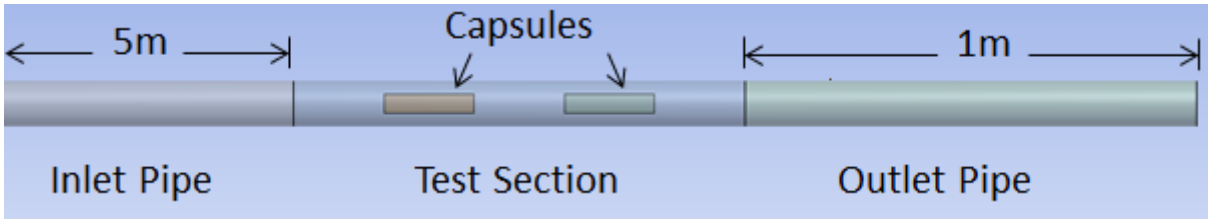

Figure 1 Schematic of the horizontal HCP

Two of the industrially most widely used 90º HCP bends of bend-to-pipe radius ratios of 4 and 8 have also been numerically modelled in the present study to analyse minor losses within HCPs, as shown in figure 2 [37].

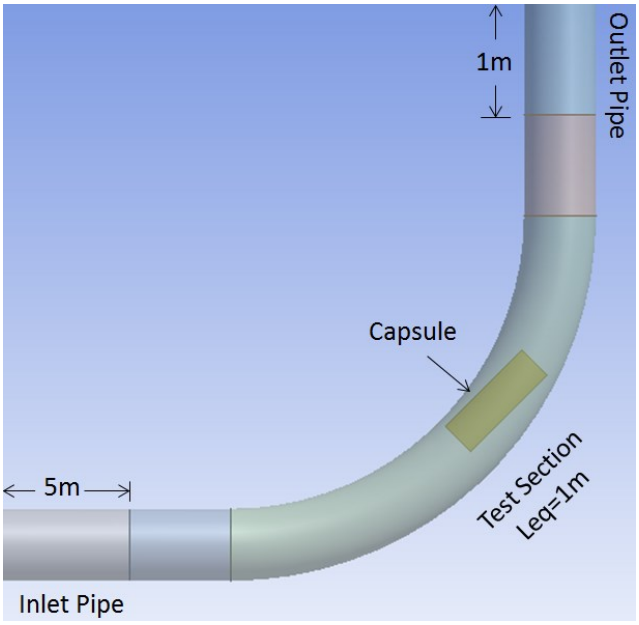

Figure 2 Schematic of an HCP Bend

A structured mesh, comprising of tetrahedral elements, has been generated for both the inlet and the outlet pipes, whereas, the test section of the pipeline has been meshed with unstructured elements due to the presence of capsules which makes the geometry complex. Two meshes, with 1,000,000 and 2,000,000 mesh elements, have been generated for spatial discretisation of the flow domain. The results obtained, shown in table 1, depict that the difference in the pressure drop across the test section of the HCP is less than 1% from the two meshes under consideration. It can therefore be concluded that the mesh with one million elements is capable of accurately predicting the complex flow phenomena within HCPs, and hence has been chosen for further analysis.

Table 1 Mesh Independence Results

Number of Mesh Elements	Pressure at Inlet (Pa)	Pressure at Outlet (Pa)	Pressure Drop per unit Length (Pa/m)	Difference in Pressure Drops (%)
1 million	11163	401	10762	0.75
2 million	11265	584	10681	

It is noteworthy that the y^+ values are such that the first mesh node is in the log-law region.

4. Boundary Conditions

The boundary types and conditions that have been used in the present study are listed in table 2. A practical range of inlet flow velocities have been considered here, corresponding to a 100mm diameter pipeline, as considered by many other researchers [9, 18-22, 26-28]. All the walls in the flow domain have been modelled using no-slip boundary condition, as is expected in real world scenarios [38-39].

Table 2 Boundary Conditions

Boundary Name	Boundary Type	Boundary Conditions
Inlet to the Pipe	Velocity Inlet	1–4m/sec
Outlet of the Pipe	Pressure Outlet	0Pa(g)
Wall of the Pipe	Stationary Wall	No-Slip
Capsules	Moving Walls	From DPM

4.1 Capsule Velocity in an HCP

The flow of capsules in an HCP is quite complicated to model as the velocity and trajectory of the capsules are not known in advance. In order to specify the capsule velocity as boundary condition in the solver, a novel modelling technique, called Discrete Phase Model (DPM), has been used in the present study to numerically compute the velocities (and trajectories) of particles within an HCP, except for heavy-density rectangular capsules in a horizontal HCP. For this particular case, Agarwal's data has been used [13]. A comparison between Agarwal's data and the capsules' velocities predicted by DPM has been presented in figure 3 showing that the DPM predicts capsules' velocities with reasonable accuracy.

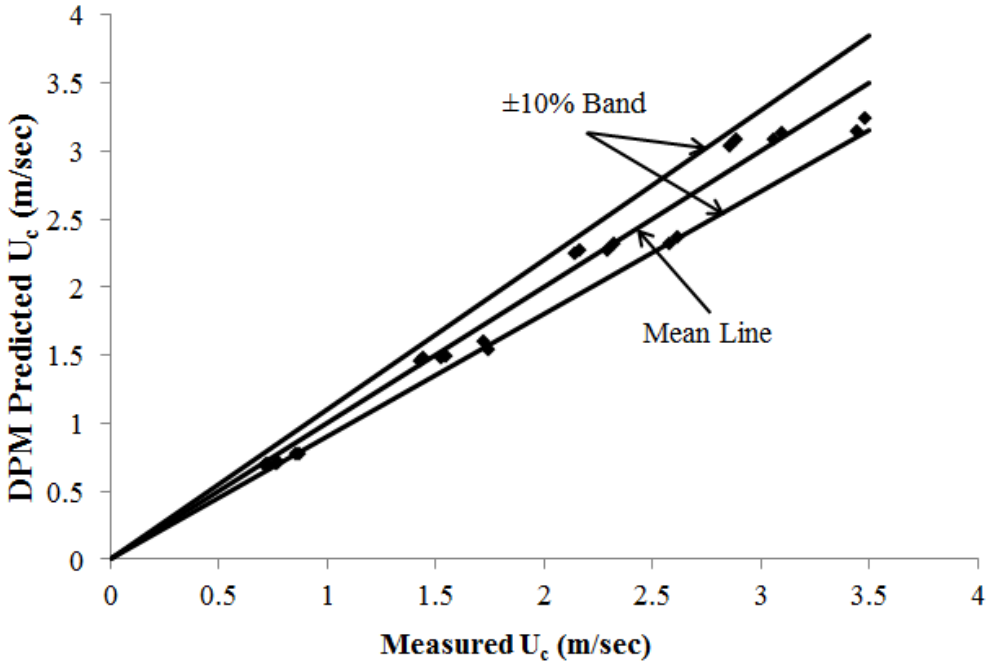

Figure 3 Comparison between Agarwal's measured U_c and DPM's predicted U_c for the flow of heavy-density rectangular capsules in horizontal HCPs

For more realistic numerical modelling, the shape and size of the particles used in the DPM are identical to the capsules considered. The shape of the particles has been defined using the shape factor (Ψ), which can be represented as:

$$\Psi = \frac{Surface\ area\ of\ a\ sphere\ having\ the\ same\ volume\ as\ the\ capsule}{Actual\ surface\ area\ of\ the\ capsule} \quad (10)$$

DPM solves transport equations for the continuous phase, i.e. water in case of hydraulic capsule bends. It also allows simulating a discrete second phase in a Lagrangian frame of reference [40]. This second phase consists of rectangular particles dispersed in the continuous phase. DPM computes the velocities and trajectories of these discrete phase entities. The

coupling between the phases and its impact on both the discrete phase velocities and trajectories, and the continuous phase flow has been included in the present study. The discrete phase in the DPM is defined by defining the initial position and size of the capsules. These initial conditions, along with the inputs defining the physical properties of the discrete phase (capsule), are used to initiate trajectory and velocity calculations. The trajectory and velocity calculations are based on the force balance on the capsule. The trajectory of a discrete phase particle is predicted by integrating the force balance on the particle, which is written in a Lagrangian reference frame. This force balance equates the particle inertia with the forces acting on the particle, and can be written as:

$$\frac{dU_{pr}}{dr} = D_F\,(U_w - U_{pr}) + \frac{g\,(\rho_{pr}-\rho_w)}{\rho_{pr}} \tag{11}$$

where U_{pr} and U_w are the velocities of particles and water respectively, ρ_{pr} and ρ_w are the densities of particles and water respectively, r is time and g is the gravitational acceleration. $D_F(U_w\text{-}U_{pr})$ is the drag force per unit particle mass, where the drag force can be re-written as:

$$D_F = \frac{1}{2}\,\rho_w\left(U_w - U_{pr}\right)^2 A\,C_d \tag{12}$$

where C_d is the drag coefficient and A is the cross-sectional area of the particle:

$$D_F = \frac{1}{2}\,Re_{pr}\left(U_w - U_{pr}\right)\frac{\pi d_{pr}\mu}{4}\,C_d \tag{13}$$

where d_{pr} is the particle's hydraulic diameter.

$$D_F\,(U_w - U_{pr}) = \frac{\frac{1}{2}Re_{pr}\left(U_w - U_{pr}\right)\frac{\pi d_{pr}\mu}{4}C_d}{\frac{\pi {d_{pr}}^3}{6}\rho_{pr}} \tag{14}$$

$$D_F = \frac{3\,\mu\,C_d\,Re_{pr}}{4\,\rho_{pr}\,{d_{pr}}^2} \tag{15}$$

where Re_{pr} is the Reynolds number of the particle/s. In the present study, Saffman's lift force due to shear has also been included in the study as an additional force acting on the particles [41].

In the case of capsule flow in HCP bends, the velocity of rectangular capsules is assumed to be a function of capsule's location within the bend. In order to investigate the likely influence of the angular position of rectangular capsules within HCP bends, detailed analysis has been carried out at six equally spaced angular positions (θ) of 0º, 18º, 36º, 54º, 72º and 90º to cover a wide range of analysis. After conducting some preliminary investigations, it has been observed that the pressure drop in an HCP bend transporting rectangular capsules is independent of the angular position of the capsule, where the density of the capsules is equal to that of water. However, the pressure drop is significantly different, at different locations, in case of the flow of heavy-density rectangular capsules in HCP bends. Hence, an average pressure drop has been considered for the analysis of the flow of heavy-density rectangular capsules in HCP bends. The average percentage error in pressure drop estimation has been computed to be less than 5%.

5. Scope of Numerical Investigations

As there are a large number of geometrical and flow related variables associated with the flow of rectangular capsules in pipelines, a Full Factorial based Design of Experiments (DoE) has been employed in the present study to determine the possible practical combinations of these parameters. A full factorial design measures responses for all combinations of the factor levels. The number of runs necessary for a full factorial design is l^f where l and f are the number of levels and factors [42]. Minitab 17 Statistical Software has been employed for this purpose, where a practical range of different parameters has been specified. The factors/parameters considered for the flow of rectangular capsules in HCPs, along with their levels, have been summarised in table 3. It can be seen that the current investigations not only consider the flow of a single capsule in HCPs (N=1), but a capsule train as well, where the train consists of upto two rectangular capsules (N=2). Three different lengths of the capsules (Lc) have been considered i.e. $1d_h$, $3d_h$ and $5d_h$, d_h being the hydraulic diameter of the capsules. Capsule-to-pipe hydraulic diameters ratios of 0.4 and 0.5 have been considered in the present study, while average flow velocities of up to 4m/sec have been specified. The spacing between the capsules (S), in a capsule train, has been varied as $1d_h$, $3d_h$ and $5d_h$. Furthermore, bend-to-pipe radius ratios (R/r) of 4 and 8, representing the most common industrial pipe bends, have been used in the present study. Moreover, both equi-density (having specific gravity s of 1) and heavy-density rectangular capsules (s=2.7 for aluminium capsules) have been numerically analysed.

Table 3 Factors and Levels for Full Factorial Design of an HCP

Factor	Level 1	Level 2	Level 3	Level 4
N/L_p	1	2	N/A	N/A
L_c	$1d_h$	$3d_h$	$5d_h$	N/A
k	0.4	0.5	N/A	N/A
U_{av}	1	2	3	4
S	$1d_h$	$3d_h$	$5d_h$	N/A
R/r	4	8	N/A	N/A
s	1	2.7	N/A	N/A

The resulting numbers of numerical simulations, which are equal to 576, have been carried out, and the pressure drop per unit length of the pipeline has been recorded for each simulation. Novel semi-empirical prediction models, similar to equations (5-6 and 8-9), have then been developed for the friction factor and loss coefficient of capsules. These semi-empirical prediction models have then been embedded into the least-cost principle based optimisation methodology developed in the present study for rectangular capsules.

7. Verification of CFD results

Numerical predictions need to be verified against the experimental results in order to gain confidence on these predictions. Furthermore, appropriate solver settings, such as boundary conditions, turbulence modelling, interpolation schemes etc., need to be specified to the numerical simulations for accuracy in predictions. After successful verification of numerical predictions, the same solver settings can then be used for further analysis/investigations. In the present study, verification of CFD predictions regarding the pressure drop within an HCP has been carried out against the experimental results of Ulusarslan [43]. Table 4 summarises the benchmarking parameters used for the verification purposes.

Table 4 Benchmarking parameters

Name/Property	Value/Range/Comment
s	0.87
k	0.8
U_{av}	0.2–1 m/sec
N/L_p	Depending on concentration

Three dimensional Navier-Stokes equations, along with the continuity equation, have been numerically solved for the turbulent flow of water, with rectangular capsules waterborne, in a horizontal HCP. Pressure drop predictions from the CFD analysis, across the HCP, have been compared against the experimental results, as shown in figure 4. It can be seen that the pressure drop within the HCP changes as a typical power law. It can be further noticed that the CFD predicted pressure drop values are in close agreement with the experimental results, with an average variation of less than 5% for all solid phase concentrations (con.). It can thus be concluded that the numerical model considered in the present study represent the physical model of an HCP carrying rectangular capsules.

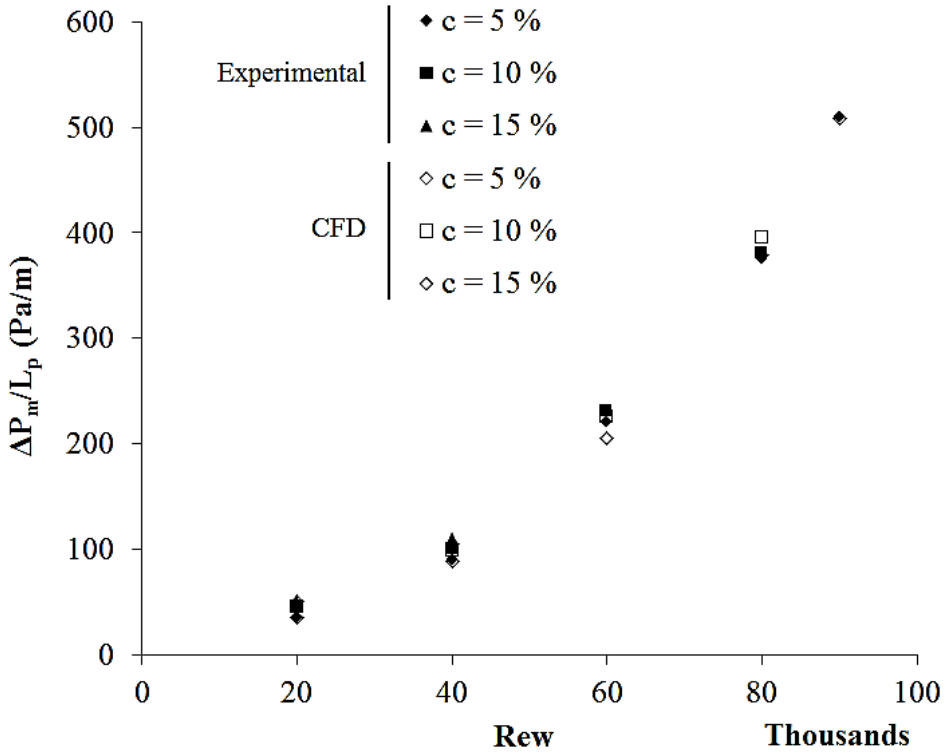

Figure 4 Comparison between CFD predicted and experimentally recorded pressure drop within an HCP

8. Results and Discussion

The literature review regarding the flow of rectangular capsules in HCPs has revealed that in-depth flow field analysis in such pipelines is extremely limited. Hence, in the present study, a detailed discussion on the complex flow structure within HCPs transporting rectangular capsules has been presented. The dependence of pressure drop across such pipelines on the various geometric and flow related variables (such as the concentration of the capsules, spacing between the capsules, average flow velocity, size of the capsules, inclination of the pipeline etc.) has been quantified. This information has then been used to develop novel

statistical prediction models for the pressure drop across the HCPs. These prediction models are fed into a design methodology for HCPs transporting rectangular capsules, in order to obtain the optimal pipeline sizing based on the specified requirements. Furthermore, a design example has been presented to show the usefulness of this study.

The simplest case, with which comparisons can be made later on, is the flow of a single rectangular capsule in a hydraulic pipeline. Figure 5 depicts the local variations in the static pressure, velocity and vorticity magnitude within a horizontal pipe, transporting a single equi-density rectangular capsule of capsule-to-pipe hydraulic diameter ratio of 0.4 at an average flow velocity of 1m/sec. The length of the capsule considered here is equal to the hydraulic diameter of the capsule. This is also the first case identified after carrying out the DoE studies.

It can be seen in figure 5(a) that the presence of a capsule makes the static pressure distribution highly non-uniform within the HCP, as compared to single phase flow where it is known that static pressure remains constant along the radial direction at a particular pipe cross-section [44]. The pressure gradients are fairly large upstream of the capsule. The higher upstream static resistance offered by the capsule to the flow. The flow then enters the annulus region between the pipe wall and the capsule. As the cross-sectional area decreases, the flow accelerates, resulting in reduction in the static pressure. The flow, while exiting the annulus region, decelerates, resulting in increase in the static pressure. Here, the shear layers roll-up due to velocity gradient, forming vortices, which are being shed into the wake of the capsule, as depicted in figure 5(c). The vortices shed downstream the capsule grow in size initially, taking their energy from the shear layers, through their trailing jets. This has been observed and explained in more detail by Gharib et al [45-48]. Once enough amount of energy has been transferred to the vortices, they detach themselves from the shear layers and travel further downstream, constantly expanding in size and dissipating their energy, leading to their eventual decay. The flow then recovers rapidly from the effects of the presence of capsule within the pipe and the static pressure recovers to some extent. This is associated with further reduction in the vorticity.

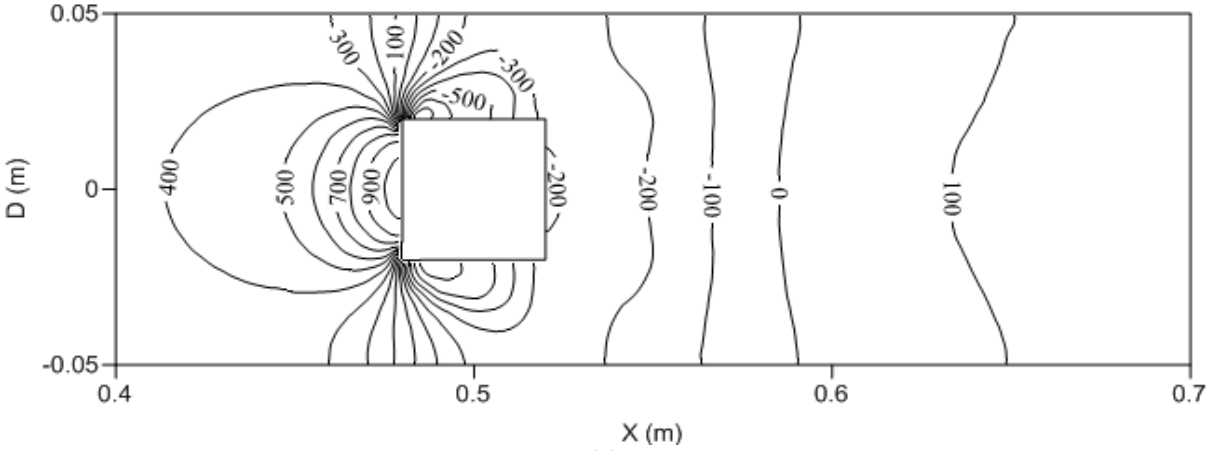

(a)

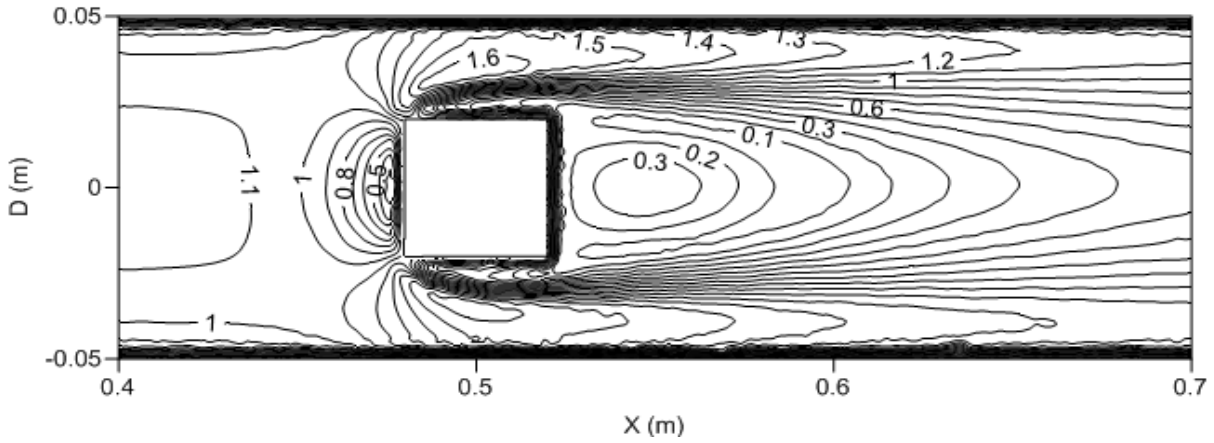

(b)

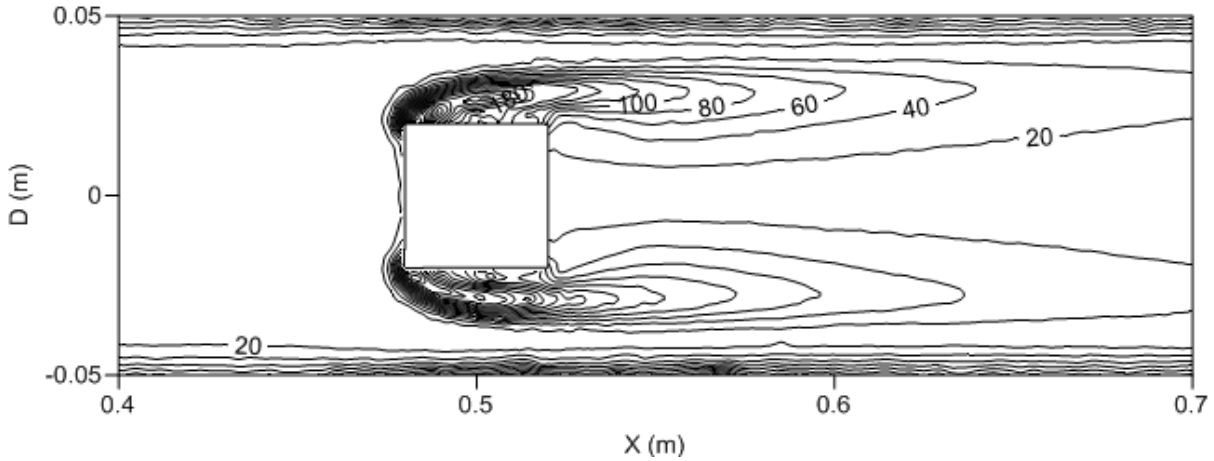

(c)

Figure 5 Flow fields within a horizontal HCP transporting a single equi-density rectangular capsule of k=0.5 and L_c=1d at U_{av}=1m/sec (a) Static pressure (Pa) (b) Velocity magnitude (m/sec) (c) Vorticity magnitude (/sec)

The drag force acting on the capsule has been computed in non-dimensional form as discussed in detail by Liu [49]. The drag coefficient has been found to be 1.79. The drag coefficient value is well within the expected range, as mentioned in the works of Feng et al [50] and Yanaida et al [51]. The pressure drop across the HCP has been calculated to be 319Pa(g) as compared to 92Pa(g) in case of water flow only. Friction factors λ_w and λ_c have been computed to be 0.0184 and 0.0454 respectively, clearly showing that the pressure drop in case of an HCP is significantly higher than a hydraulic pipeline. The values of λ_w and λ_c computed here, accommodate the changes in the parameters discussed in equations (3) and (4), and hence can be used in order to develop novel semi-empirical prediction models for the pressure drop across HCPs.

8.1 Effect of Capsule Concentration

Figure 6 depicts the local variations in the static pressure, velocity and vorticity magnitudes within the test section of the horizontal pipe, transporting a train of two equi-density rectangular capsules of capsule-to-pipe hydraulic diameter ratio of 0.4 at an average flow velocity of 1m/sec. The length of the capsule considered here is equal to the hydraulic diameter of the capsule, whereas the spacing between the capsules in the train is equal to one hydraulic diameter of the capsule. It can be seen that the static pressure distribution around the first capsule (left) is similar to the one observed in the previous case, however, it is significantly different for the second capsule (right). This indicates that the capsule-train flow

characteristics are different as compared to single-capsule flow characteristics. As compared to the previous case, when there was only one capsule present, the static pressure has slightly increased upstream of the first capsule, and is reduced further downstream. However, the static pressure variations, both upstream and downstream the second capsule, are completely different, depicting considerably less pressure drop due to the addition of the second capsule in the pipeline. Figures 6(b) and (c) suggest that the second capsule is present in the wake of the first capsule, as the velocity profile hasn't completely developed downstream the first capsule, and the shear layers are extending farther than the second capsule's front face. Due to the presence of a second capsule, which is close-by the first capsule, the shear layers on the rear peripheral face of the first capsule gets attached to the front peripheral face of the second capsule, hence vortices are not being shed downstream the first capsule. Furthermore, on the rear peripheral face of the second capsule, the energy contained within the shear layers is not enough to shed vortices. The drag coefficient of the first capsule been recorded to be 1.9, whereas the drag coefficient of the second capsule is 0.24, clearly showing that second capsule's contribution towards the pressure losses within the HCP, in this particular case, is significantly less than the first capsule.

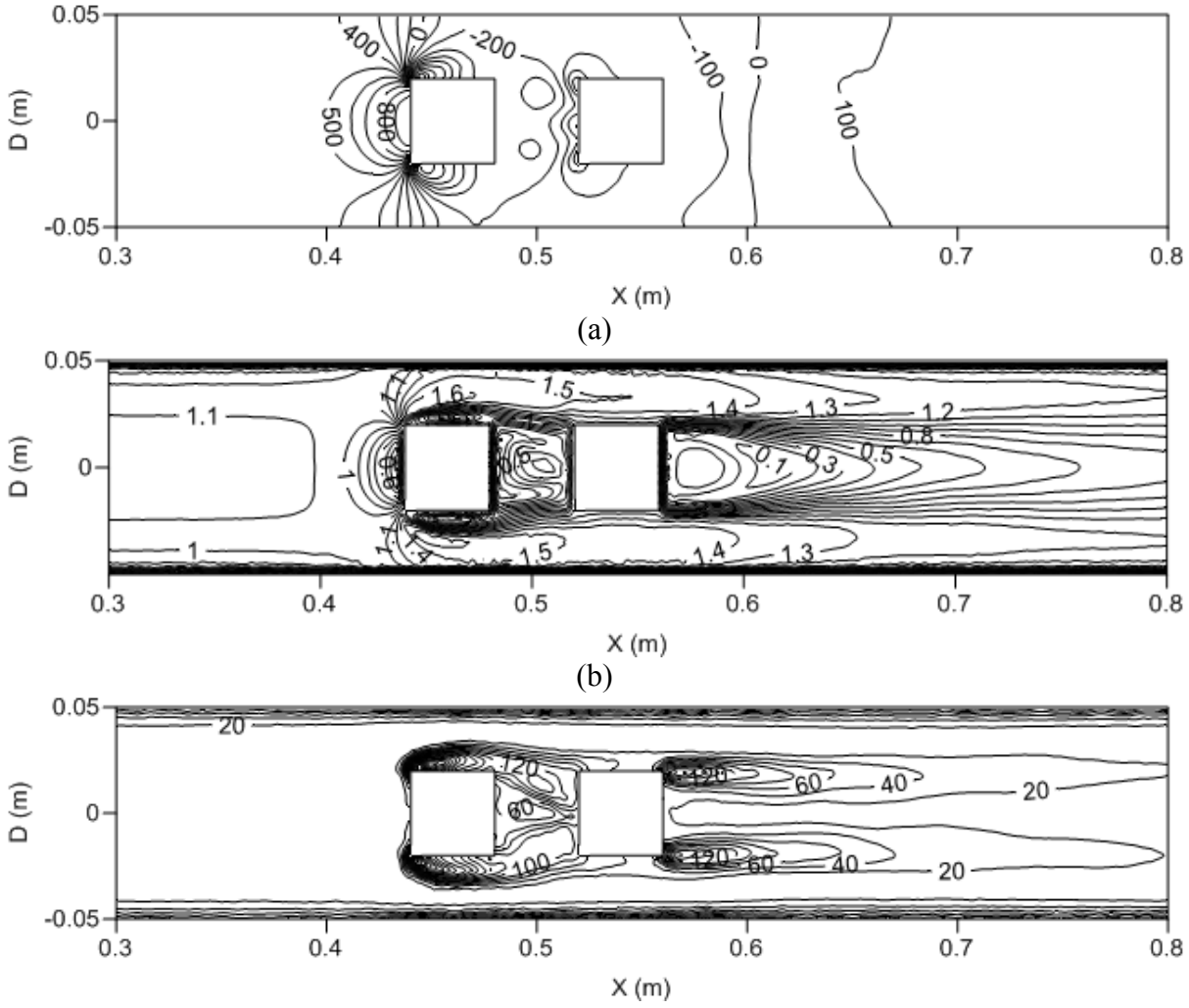

Figure 6 Flow fields within a horizontal HCP transporting two equi-density rectangular capsules of k=0.5, L_c=1d_h and S=1d_h at U_{av}=1m/sec (a) Static pressure (Pa) (b) Velocity magnitude (m/sec) (c) Vorticity magnitude (/sec)

The total pressure drop within the test section of the HCP has been calculated to be 372Pa(g), hence, λ_c is 0.056, while λ_w remains the same as discussed in the previous case. The value of fc shows that the pressure drop is higher than the previous case. It can thus be concluded that increase in the capsule concentration within an HCP increases the pressure drop within it. Moreover, two capsules that are very close-by may behave as a single long capsule within the HCP.

8.2 Effect of Capsule Spacing

Figure 7 depicts the local variations in the static pressure, velocity and vorticity magnitudes within the test section of the horizontal pipe, transporting a train of two equi-density rectangular capsules of capsule-to-pipe hydraulic diameter ratio of 0.4 at an average flow velocity of 1m/sec. The length of the capsules considered here is equal to the hydraulic diameter of the capsules, whereas the spacing between the capsules in the train is equal to five hydraulic diameters of the capsule. It can be seen in figure 7(a) that the static pressure distribution around the first capsule (left) is similar to the one observed in the previous case, however, it is significantly different for the second capsule (right). This indicates that the spacing between the capsules in an HCP is an important parameter to consider while designing HCPs. As compared to the previous case with spacing of $1d_h$ between the capsules, it can be seen that distinct vortices are being shed downstream the first capsule. This is because the second capsule is far downstream the first capsule, and hence the shear layers of the first capsule have enough energy and space to shed vortices. However, same cannot be said about the second capsule. Although the second capsule is far-off from the first one ($5d_h$ downstream the first), it has been stated by Asim [26] that a single capsule's effect can be felt up to 5d distance downstream the capsule. It can be further seen in figure 7(b) that the mixture flow velocity is still increasing before it encounters the second capsule. Hence, the second capsule's upstream effects are intersecting with first capsule's downstream effects, and the energy contained within the shear layers of the second capsule isn't enough to shed the vortices. However, this energy is enough to create one, which remains attached to its shear layers via the trailing jet.

The drag coefficient of the first capsule is 1.8, whereas it is 0.91 for the second capsule, clearly showing that the second capsule's contribution towards the pressure losses within the HCP has significantly increased in this case. A considerably higher pressure drop across the test section of the HCP is expected as the combined drag coefficients for both the capsules in the previous case was 2.14, and in the present case is 2.71.

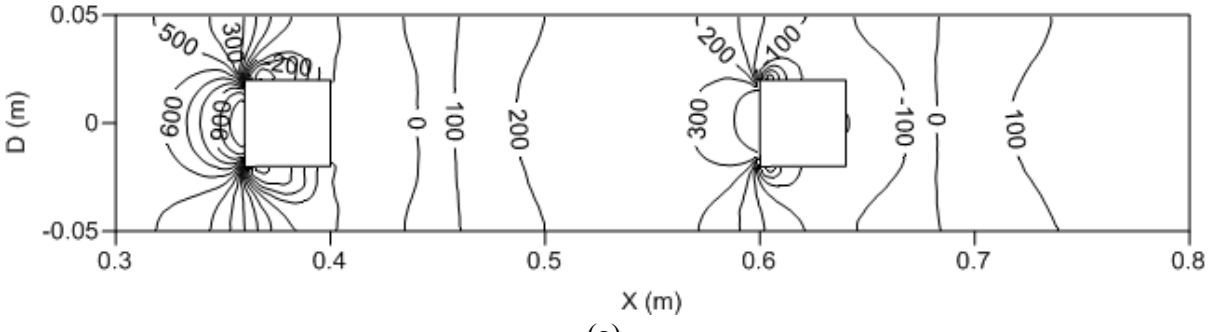

(a)

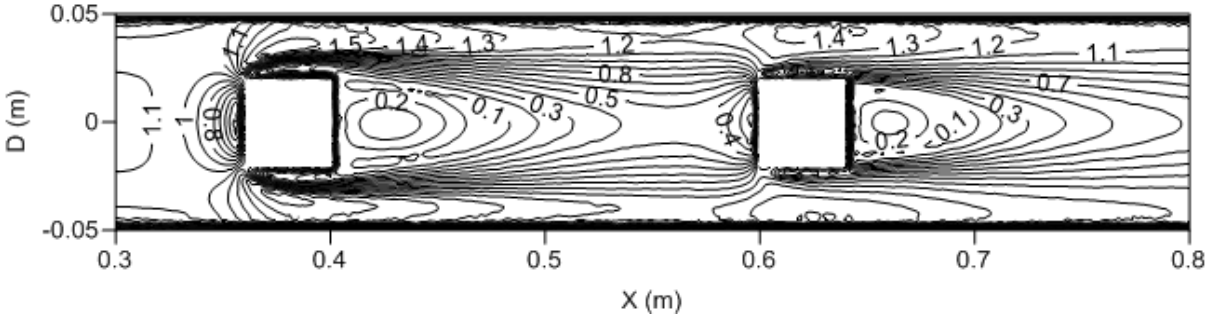

(b)

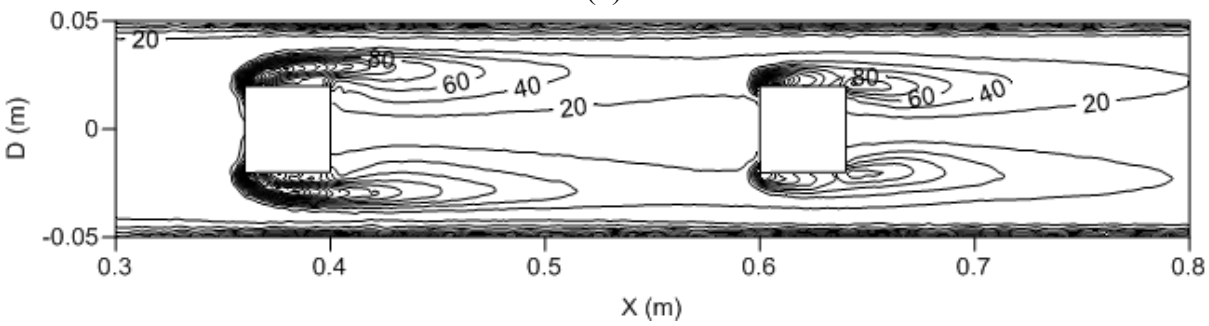

(c)

Figure 7 Flow fields within a horizontal HCP transporting two equi-density rectangular capsules of k=0.4, $L_c=1d_h$ and $S=5d_h$ at U_{av}=1m/sec (a) Static pressure (Pa) (b) Velocity magnitude (m/sec) (c) Vorticity magnitude (/sec)

The total pressure drop within the test section of the HCP has been calculated to be 435Pa(g), hence, λ_c is 0.068, while λ_w remains the same as discussed in the case of a single capsule flow. The value of fc shows that the pressure drop is higher than the previous case. It can thus be concluded that increase in the spacing between the capsules in a train, increases the pressure drop across the HCP.

8.3 Effect of Capsule Size

Figure 8 depicts the local variations in the static pressure, velocity and vorticity magnitudes within the test section of the horizontal pipe, transporting a single equi-density rectangular capsule of capsule-to-pipe hydraulic diameter ratio of 0.5 at an average flow velocity of 1m/sec. The length of the capsule considered here is equal to the hydraulic diameter of the capsule. It can be seen in figure 8(a) that the static pressure distribution is highly non-uniform within the HCP. The static pressure difference between the upstream and downstream locations of the capsules is significantly higher than observed in case of capsule-to-pipe hydraulic diameter ratio of 0.4, indicating that the pressure drop would be much higher in this case. The higher upstream static pressure is due to the larger frontal cross-sectional area of the capsule, offering more resistance to the flow of its carrier fluid within the HCP. This is further associated with the reduction in the flow velocity upstream the capsule, as depicted in figure 8(b). Same trends have been observed in case of capsule-to-pipe hydraulic diameter ratio of 0.4, with the difference of the scale only, which is expected to increase drag on the capsule. The drag coefficient in this case is 2.5, which is 39% higher than for capsule-to-pipe hydraulic diameter ratio of 0.4.

The flow then enters the annular region between the pipe wall and the capsule. As the cross-sectional area decreases, the flow accelerates (as depicted in figure 8(b)), resulting in reduction in the static pressure. This is also consistent with the observations in case of capsule-to-pipe hydraulic diameter ratio of 0.4; however, the cross-sectional area of the annulus is much smaller in the present case. It can be further noticed that vortices are being

formed downstream the capsule, and the trends in the vorticity magnitude variations are the same as observed in case of capsule-to-pipe hydraulic diameter ratio of 0.4.

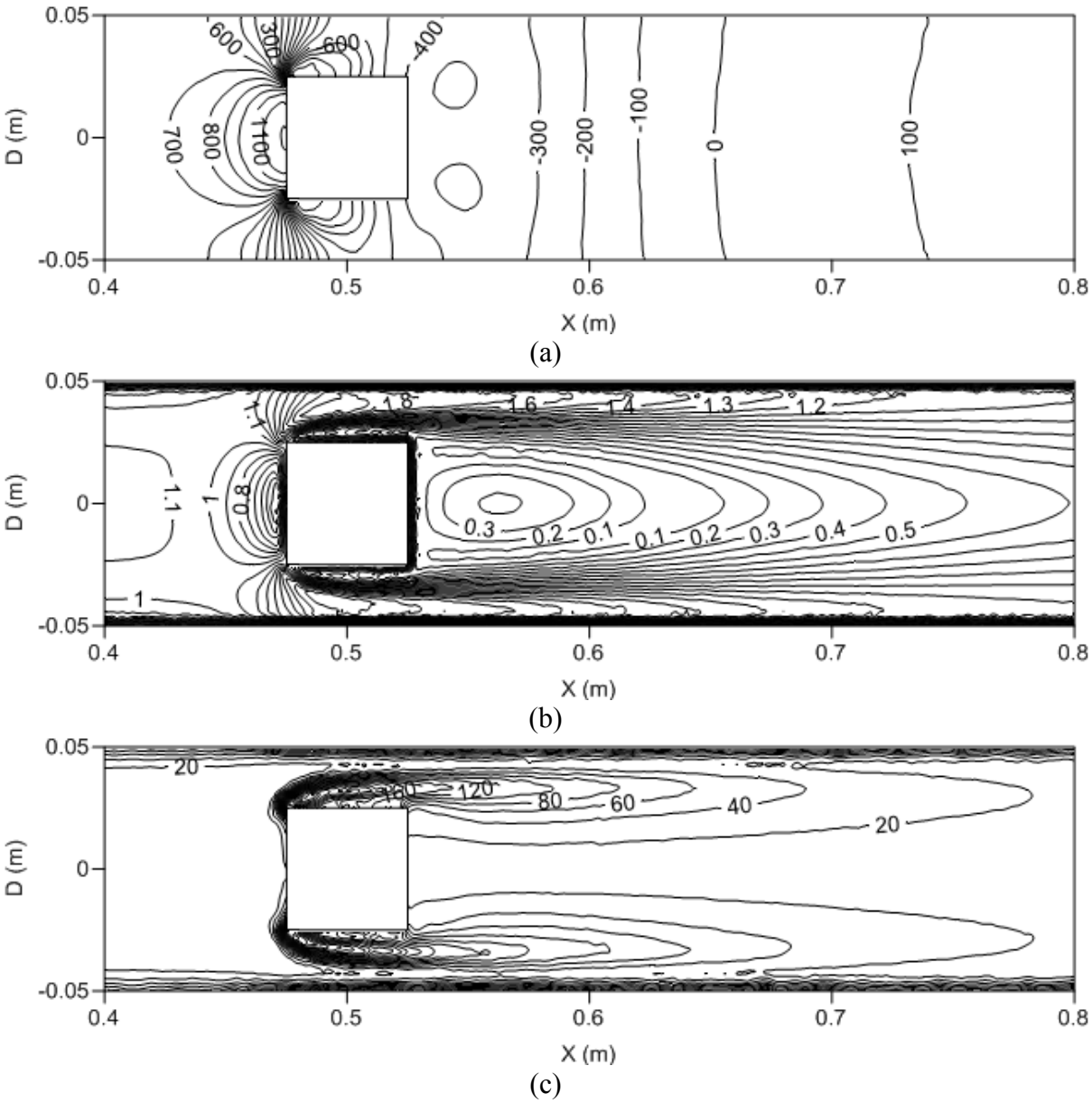

Figure 8 Flow fields within a horizontal HCP transporting a single equi-density rectangular capsule of k=0.5 and L_c=1d_h at U_{av}=1m/sec (a) Static pressure (Pa) (b) Velocity magnitude (m/sec) (c) Vorticity magnitude (/sec)

The pressure drop in this particular case is 583Pa(g), which is 83% higher than for capsule-to-pipe hydraulic diameter ratio of 0.4, hence the pressure drop within HCPs increases as the capsule-to-pipe hydraulic diameter ratio of the capsules increases. The friction factor corresponding to the capsule (λ_c) has been computed to be 0.0983, which is 116% higher than for capsule-to-pipe hydraulic diameter ratio of 0.4.

Figure 9 depicts the local variations in the static pressure, velocity and vorticity magnitudes within the test section of the horizontal pipe, transporting a single equi-density rectangular capsule of a longer length with capsule-to-pipe hydraulic diameter ratio of 0.4 at an average flow velocity of 1m/sec. The length of the capsule considered here is equal to five times the hydraulic diameter of the capsule. It can be seen in figure 9(a) that the static pressure

distribution upstream the capsule is highly non-uniform and resembles that for the capsule length of $1d_h$. These variations can be seen in the annular region as well, however, these effects are noticed only up to about $2d_h$ length of the capsule, after which no significant pressure variations are observed in the axial direction. It is noteworthy that the vortices are not being shed downstream the capsules, although they are formed by the roll-up of the shear layers, and remain attached to the capsule via their trailing jets. The reason behind this is the fact that although the shear layers have higher energy content near the front peripheral area of the capsule, the viscous effects gets dissipated along the axial direction, and by the time the flow exits the annulus region, the energy content of the shear layers have reduced below the threshold of vortex shedding i.e. the formation number, as discussed earlier. This is evident from figure 9(c) as well that the vorticity is being generated from the frontal periphery of the capsule, but due to longer capsule, it gets dissipated before it reaches the rear periphery of the capsule.

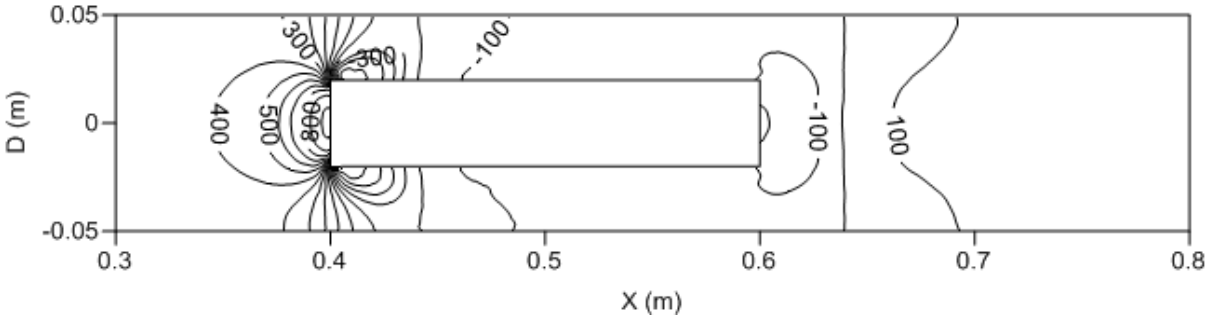

(a)

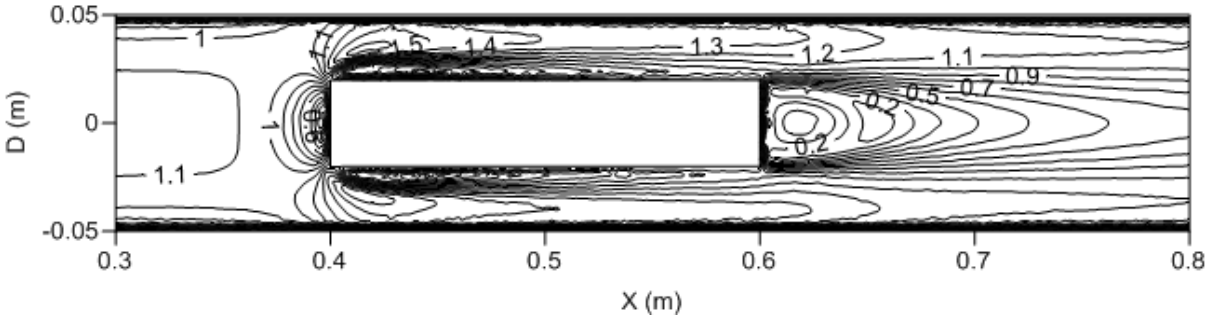

(b)

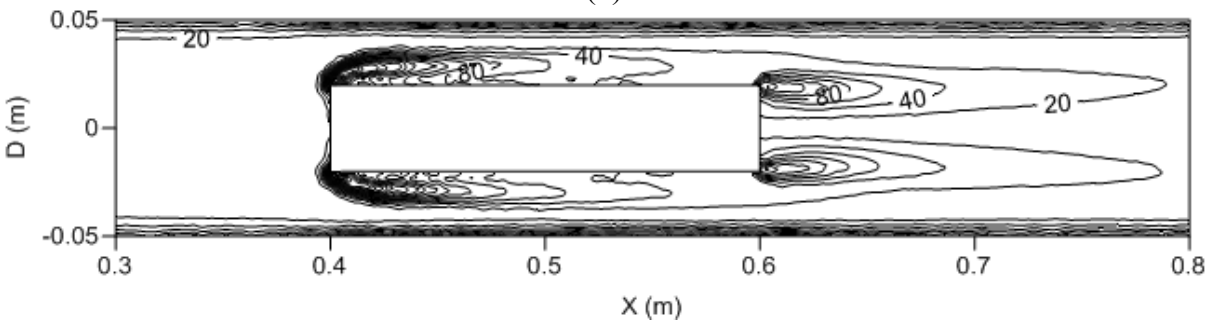

(c)

Figure 9 Flow fields within a horizontal HCP transporting a single equi-density rectangular capsule of k=0.4 and $L_c=5d_h$ at U_{av}=1m/sec (a) Static pressure (Pa) (b) Velocity magnitude (m/sec) (c) Vorticity magnitude (/sec)

The drag coefficient in this case is 1.6, which is 11% lower than for capsule length of $1d_h$, indicating that the pressure losses will be less in the present case as compared to capsule length of $1d_h$. The pressure drop across the test section of the HCP has been calculated to be

304Pa(g), which is 5% less than for capsule length of $1d_h$. The corresponding friction factor of to the capsule (λ_c) is 0.0424, which is 6.6% less than for capsule length of $1d_h$. Hence, increase in the length of the capsule, within the range considered in the present study, decreases the pressure drop within HCPs. However, the length of the capsule, within the range considered in the present study, has negligibly small effect on the pressure drop within HCPs. This means that more cargo can be transported with longer capsules at relatively lesser extra cost.

8.4 Effect of Flow Velocity

Figure 10 depicts the local variations in the static pressure, velocity and vorticity magnitudes within the test section of the horizontal pipe, transporting a single equi-density rectangular capsule of capsule-to-pipe hydraulic diameter ratio of 0.4 at an average flow velocity of 4m/sec. The length of the capsule considered here is equal to the hydraulic diameter of the capsule. It can be seen in figure 10(a) that the static pressure distribution is highly non-uniform within the HCP. The static pressure difference between the upstream and downstream locations of the capsules is significantly higher than observed in case of capsule flow with average water flow velocity of 1m/sec, as expected from equation (5), indicating that the pressure drop would be significantly higher. The pressure variations observed here are consistent with the trends observed in case of average flow velocity of 1m/sec, with the difference of the scale only, however, the non-dimensional pressure drag coefficient is not expected to increase because of the same frontal area of the capsule. The drag coefficient in this case is 1.81, which is almost the same as for average flow velocity of 1m/sec. Furthermore, figures 10(b) and (c) depicts higher flow velocities and higher vorticity magnitude within the test section of the HCP, which is again due to higher average flow velocity and hence non-dimensional analysis, becomes ever more important in this case.

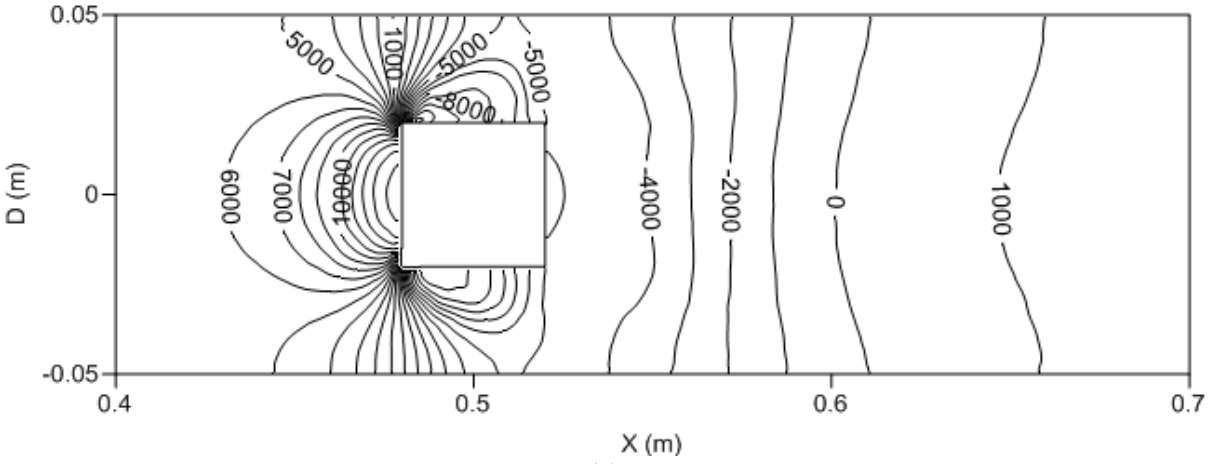

(a)

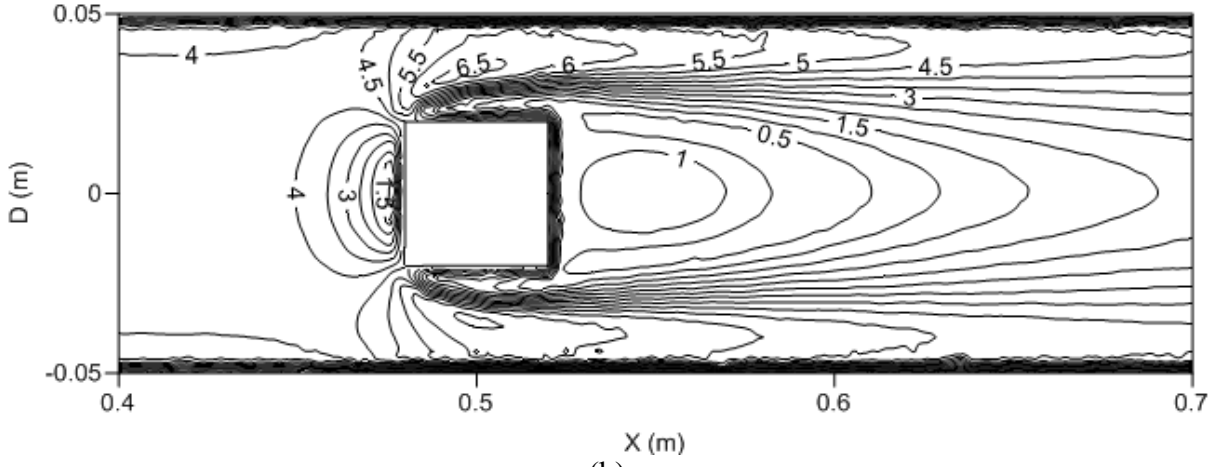

(b)

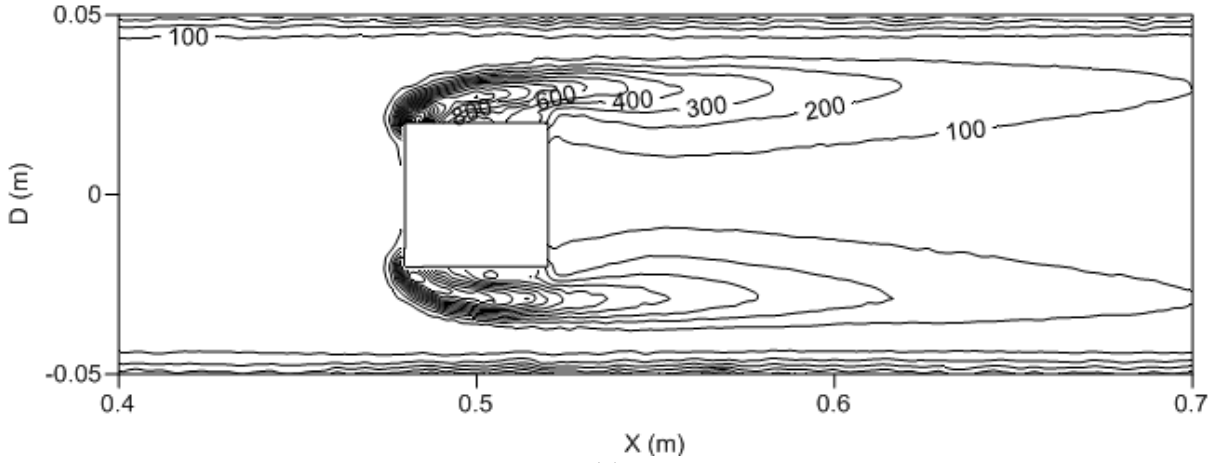

(c)

Figure 10 Flow fields within a horizontal HCP transporting a single equi-density rectangular capsule of k=0.4 and L_c=1d_h at U_{av}=4m/sec (a) Static pressure (Pa) (b) Velocity magnitude (m/sec) (c) Vorticity magnitude (/sec)

The pressure drop in this particular case is 4635Pa(g), which is 13.5 times higher than for average flow velocity of 1m/sec, hence the pressure drop within HCPs increases as the average flow velocity increases. The friction factors λ_w and λ_c have been computed to be 0.0138 and 0.044 respectively. A lower λ_w was expected, as it is an established fact that as Reynolds number of a single phase flow increases, λ_w decreases [52].

8.5 Effect of Capsule Density

Figure 11 depicts the local variations in the static pressure, velocity and vorticity magnitudes within the test section of the horizontal pipe, transporting a single heavy-density rectangular capsule of capsule-to-pipe hydraulic diameter ratio of 0.4 at an average flow velocity of 1m/sec. The length of the capsule considered here is equal to the hydraulic diameter of the capsule. It can be seen in figure 11(a) that because the capsule is heavier than its carrier fluid; it propagates along the bottom wall of the pipe. The static pressure distribution is highly non-uniform within the HCP with areas of recirculation both upstream and downstream the capsule. Furthermore, it can be seen that the effect of the capsule is felt much farther downstream the capsule. This deviation in the flow field is expected to generate more secondary flows, as can be observed in figure 11(c), indicating more losses in the pipeline. The drag coefficient has been computed to be 1.9, which is 5.5% higher than the drag coefficient of an equi-density rectangular capsule. Furthermore, the pressure drop calculated

across the test section is 328Pa(g), which is 2.8% higher than for an equi-density rectangular capsule. The pressure drop is slightly higher in case of heavy-density rectangular capsules because of the secondary flows downstream the capsule, which disrupts the flow, hence extracting energy from it.

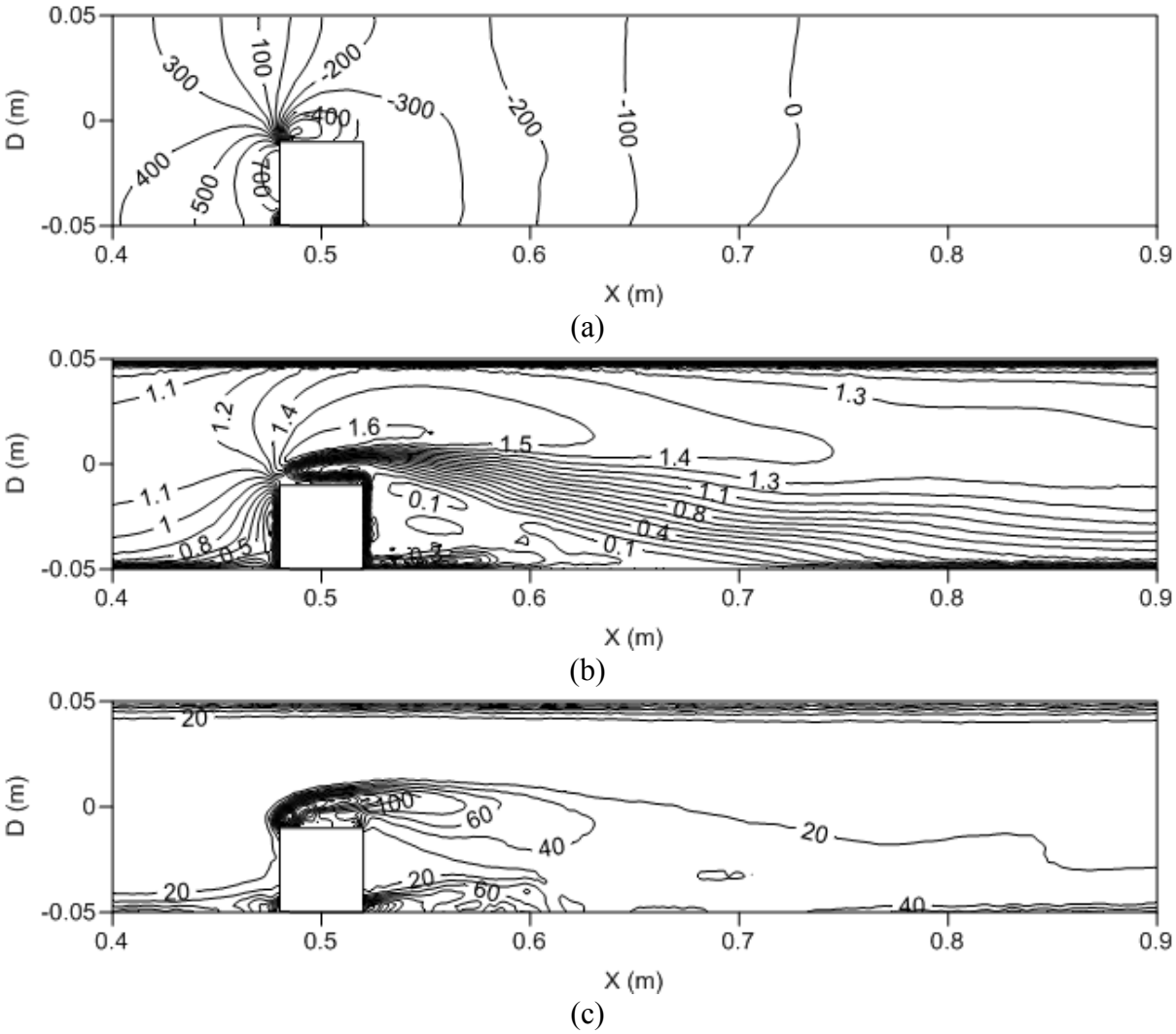

Figure 11 Flow fields within a horizontal HCP transporting a single heavy-density rectangular capsule of k=0.4 and L_c=1d_h at U_{av}=1m/sec (a) Static pressure (Pa) (b) Velocity magnitude (m/sec) (c) Vorticity magnitude (/sec)

The friction factor for capsules (λ_c) has been computed to be 0.0473, which is 4.1% higher than for an equi-density rectangular capsule, indicating the heavy-density capsule is contributing more towards the pressure drop within the HCP as compared to an equi-density capsule.

8.6 Effect of Pipe's Inclination

Pipelines mostly used in off-shore installations comprise of vertical pipes and pipe fittings. In order to cover a wide range of applications for HCPs, vertical HCP pipes have also been considered in the present investigation. Figure 12 depicts the local variations in the static pressure, velocity and vorticity magnitudes within the test section of the vertical pipe, transporting a single equi-density rectangular capsule of capsule-to-pipe hydraulic diameter ratio of 0.4 at an average flow velocity of 1m/sec. The length of the capsule considered here

is equal to the hydraulic diameter of the capsule. It can be seen that the flow fields in a vertical HCP resembles that of a horizontal HCP for the flow of equi-density rectangular capsules. While heavy-density rectangular capsules slide along the bottom wall of a horizontal HCP, they travel along the central axis of the vertical HCP. Hence, the flow of heavy-density rectangular capsules in vertical HCPs also resembles the flow of equi-density rectangular capsules in both horizontal and vertical HCPs. Furthermore, it can be visualised in figure 12(a) that the effects of the capsule are limited to a very small distance downstream the capsule.

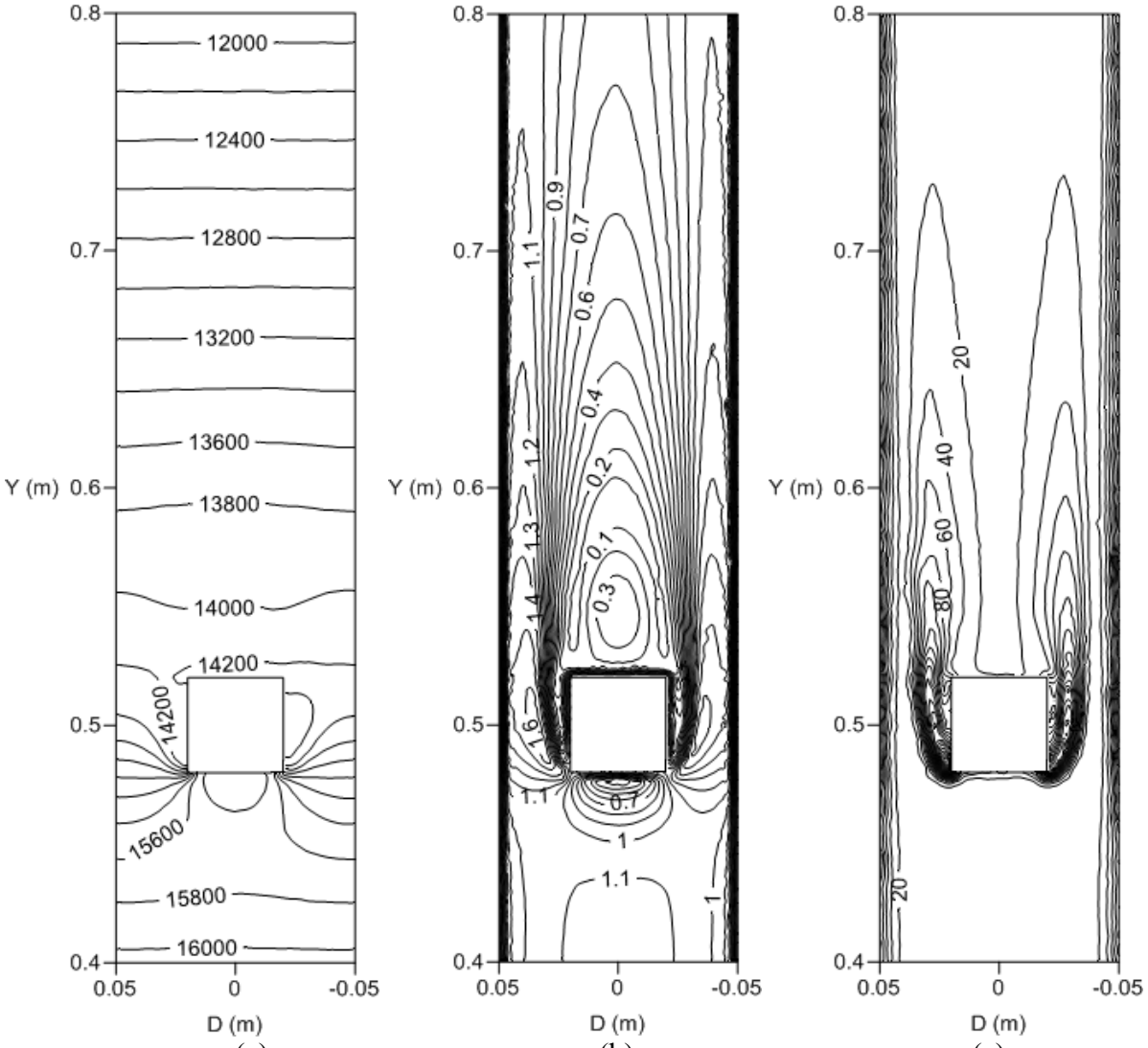

Figure 12 Flow fields within a vertical HCP transporting a single equi-density rectangular capsule of k=0.4 and L_c=1d_h at U_{av}=1m/sec (a) Static pressure (Pa) (b) Velocity magnitude (m/sec) (c) Vorticity magnitude (/sec)

From equation (6), it is expected that due to the elevation of the pipeline there will be additional pressured drop as compared to a horizontal pipeline. The same has been observed in case of a vertical HCP, where the pressure drop across the test section of the vertical HCP is significantly higher than for a horizontal HCP. After carrying out detailed quantitative analysis, it has been found out that the higher pressure drop within a vertical HCP is due to the elevation of the pipeline only, and the contribution of the capsule towards the pressure drop across a vertical HCP is the same as in case of a horizontal HCP. This is further

summarised in table 5 which shows the pressure drop contribution in the two pipelines (horizontal and vertical) by the capsule only. Hence, it can be concluded that equi-density rectangular capsules, either in a horizontal or vertical pipelines, contributes the same pressure drop; however, the same cannot be stated about the heavy-density rectangular capsules, as the flow behaviour in the two pipelines would be altogether different.

Table 5 Pressure drop comparison, due to a single equi-density rectangular capsule only, in Horizontal and Vertical HCPs

k	U_{av}	ΔP_c (Horizontal Pipe)	ΔP_c (Vertical Pipe)
0.4	1	227	234
0.4	2	889	905
0.4	3	1932	2005
0.4	4	3531	3501
0.5	1	491	496
0.5	2	1933	1933
0.5	3	4264	4263
0.5	4	7612	7596

Due to significantly higher mixture pressure at the rear end of the capsule, as compared to a horizontal HCP, the effects of the capsules are limited to a very small distance downstream the capsule. Although there is an indication of very less energy vortices being developed at the rear end of the capsule, however, they remain attached to the rear end of the capsule, and get dissipated very quickly. The mixture pressure keeps on decreasing linearly almost throughout the test section of the HCP, with a sudden decrease at the location where the capsule is located. The drag coefficient of the capsule is 2.55, which is 41.6% higher than in a horizontal HCP. Capsule friction factor (λ_c) has computed to be 0.0468 in this case, which is marginally higher than in a horizontal HCP.

8.7 Capsule Flow in Bends

Minor losses in the pipeline cannot be neglected while designing a pipeline, which is true for HCPs as well. Hence, a detailed investigation on HCP bends has been included in the present study, which is of utmost importance to the pipeline designers as the availability of this information is very limited in the literature. Figure 13 depicts the local variations in the static pressure, velocity and vorticity magnitudes within a horizontal HCP bend of bend-to-pipe radius ratio of 4 carrying a single equi-density rectangular capsule of capsule-to-pipe hydraulic diameter ratio of 0.4 at an average flow velocity of 1m/sec. The length of the capsule considered here is equal to the hydraulic diameter of the capsule. It can be seen in figure 13(a) that the pressure distribution within an HCP bend is altogether different to the one observed in case of a straight HCP, due to the curvature of the pipeline and the location of the capsule within the bend. Although the pressure distribution is somewhat similar upstream the capsule, it is very different downstream it. The secondary flow generating capability within an HCP is considerably more; with many recirculating zones present downstream the capsule. Hence, the losses within an HCP bend, as compared to a straight HCP, are more, which is also true for hydraulic pipelines [53].

The velocity (figure 13(b)) downstream the capsule have been observed to be varying till the end of the bend, and similar trends are noticed in case of vorticity magnitude distribution as well (figure 13(c)). Because the capsule, at this particular location and orientation within the HCP bend, is nearer to the bottom wall of the bend, uneven vortices are being shed from either ends of the capsule, downstream it.

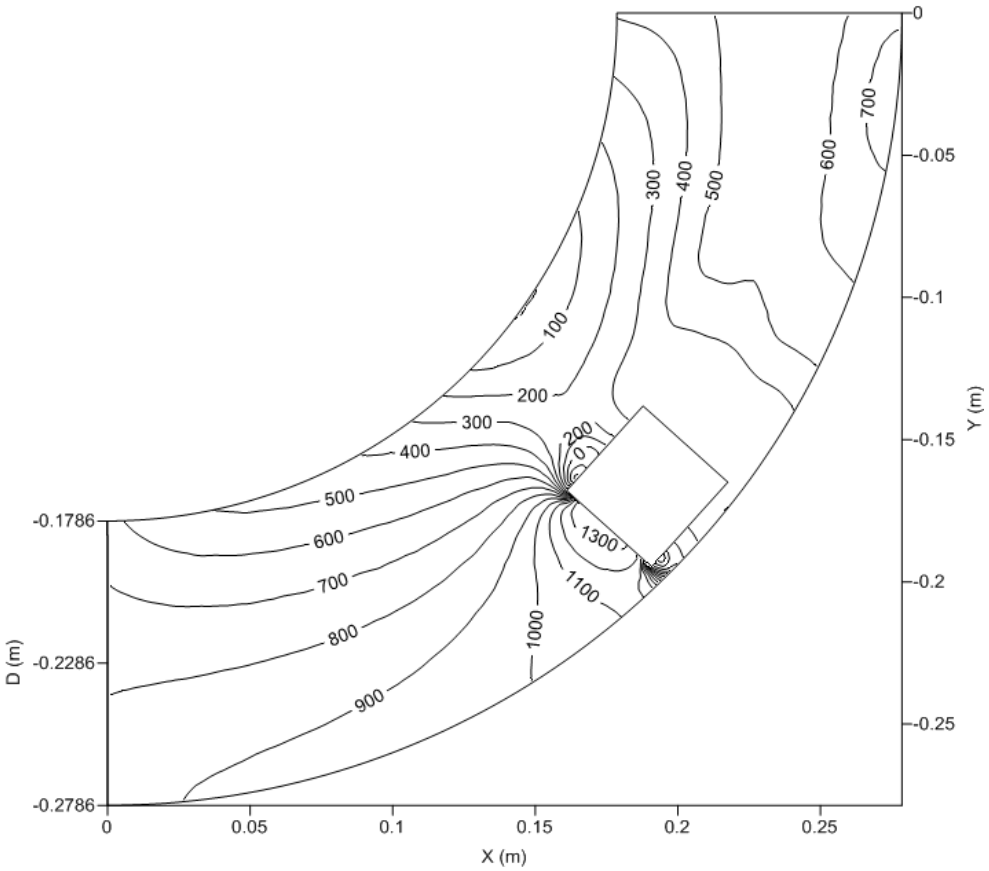
0
-0.05
-0.1
-0.15
-0.2
-0.25
Y (m)
-0.1786
-0.2286
-0.2786
D (m)
0
0.05
0.1
0.15
0.2
0.25
X (m)
100
200
300
400
500
600
700
800
900
1000
1100
1300

(a)

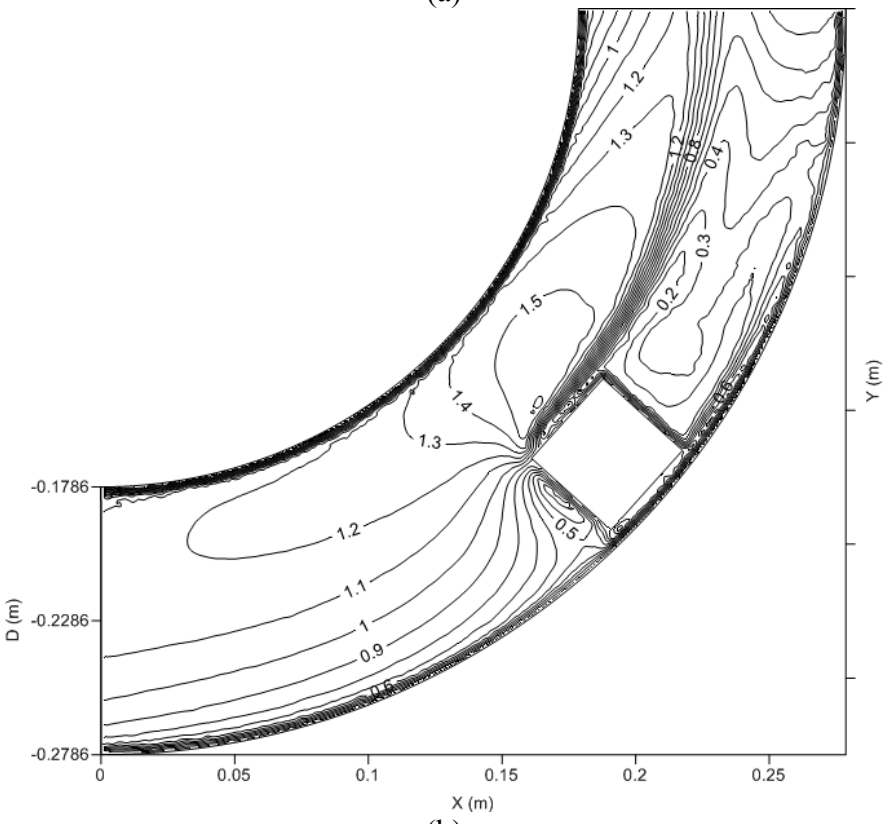
-0.1786
-0.2286
-0.2786
D (m)
0
0.05
0.1
0.15
0.2
0.25
X (m)
Y (m)
1
1.2
1.3
1.4
1.5
1.2
1.1
1
0.9
0.8
0.6
0.4
0.3
0.2
0.5

(b)

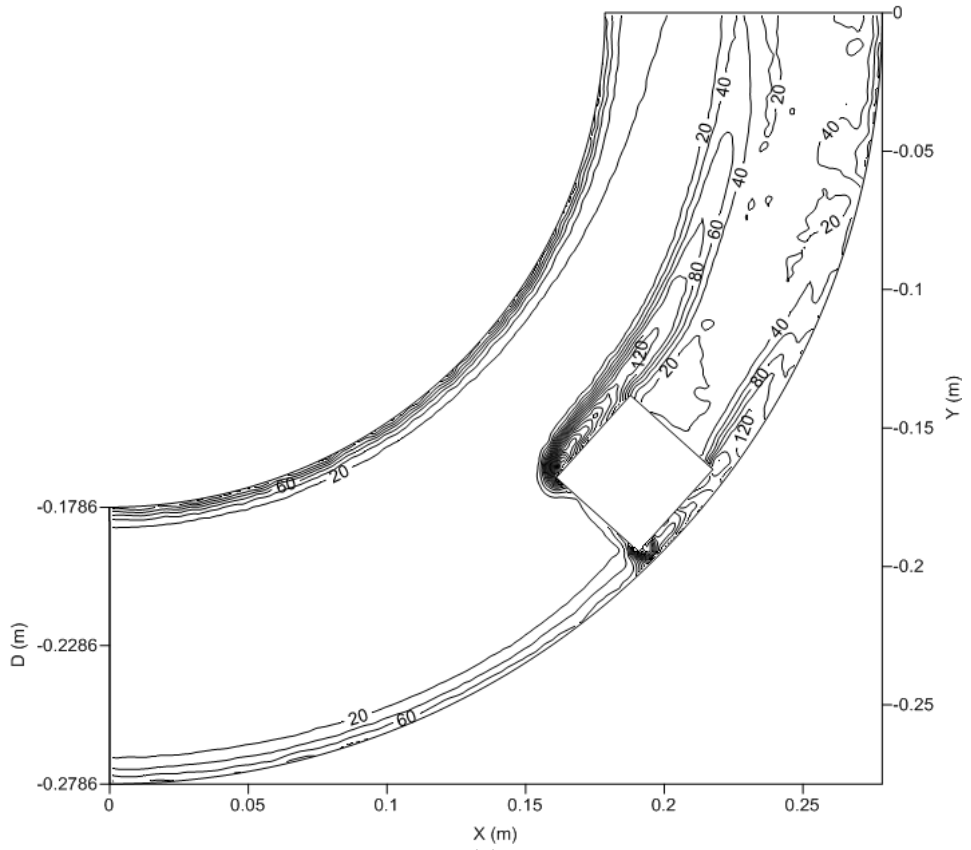

(c)

Figure 13 Flow fields within a horizontal 90º HCP bend of R/r=4, transporting a single equi-density rectangular capsule of k=0.4 and L_c=1d_h at U_{av}=1m/sec (a) Static pressure (Pa) (b) Velocity magnitude (m/sec) (c) Vorticity magnitude (/sec)

The pressure drop in this particular case is 437Pa(g), which is 37% higher than the pressure drop within a horizontal pipeline carrying rectangular capsule of the same size. Ω_c has been computed to be 0.611 in the present case. Ω_c has later been used to develop semi-empirical novel expressions to accommodate the minor losses within HCPs, for design purposes.

8.8 Effect of Curvature of the Bend

Figure 14 depicts the local variations in the static pressure, velocity and vorticity magnitudes within a horizontal HCP bend of bend-to-pipe radius ratio of 8 carrying a single equi-density rectangular capsule of capsule-to-pipe hydraulic diameter ratio of 0.4 at an average flow velocity of 1m/sec. The length of the capsule considered here is equal to the hydraulic diameter of the capsule. It can be seen in figure 14(a) that the pressure distribution is somewhat similar to the one observed in the previous case; however, the variations in the static pressure downstream the capsule are more subtle. This is because the radius of curvature of the bend in the present case is more; hence it resembles more to a straight pipe, as compared to the previous case. This implies that the secondary flow generating capability within this bend is considerably less, with no distinct recirculating zone observed downstream the capsule. The velocity profiles downstream the capsule have been observed to be varying till the end of the bend, while vorticity profiles are contained within a finite distance downstream the capsule.

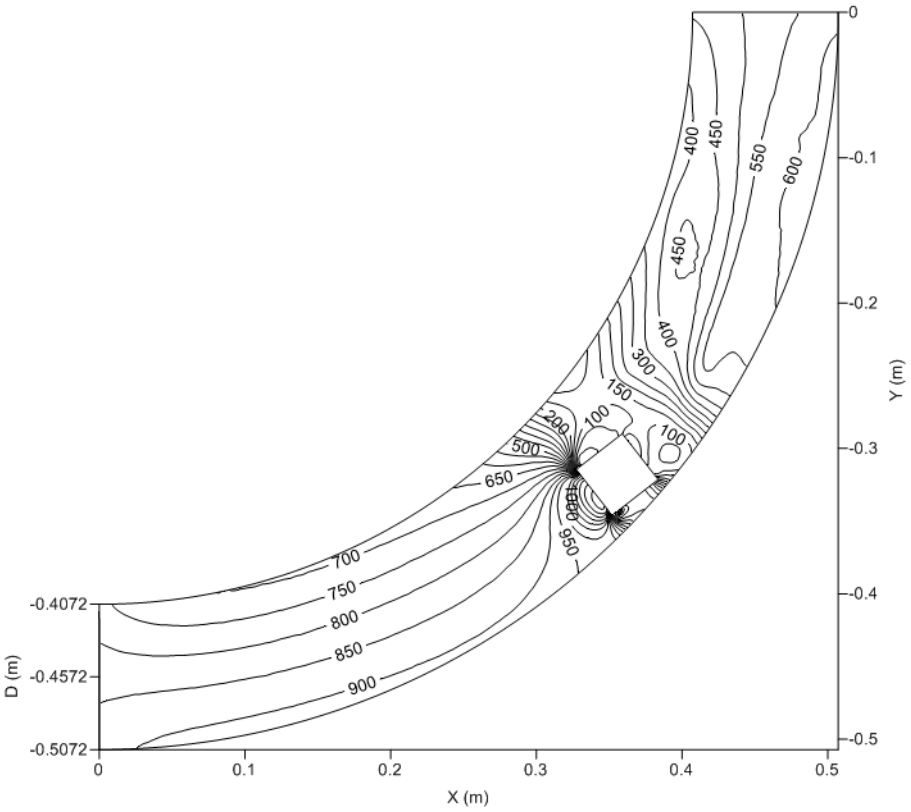
D (m)
-0.4072
-0.4572
-0.5072
X (m)
0
0.1
0.2
0.3
0.4
0.5
Y (m)
-0.1
-0.2
-0.3
-0.4
-0.5
700
750
800
850
900
950
650
500
200
100
150
300
400
450
550
600

(a)

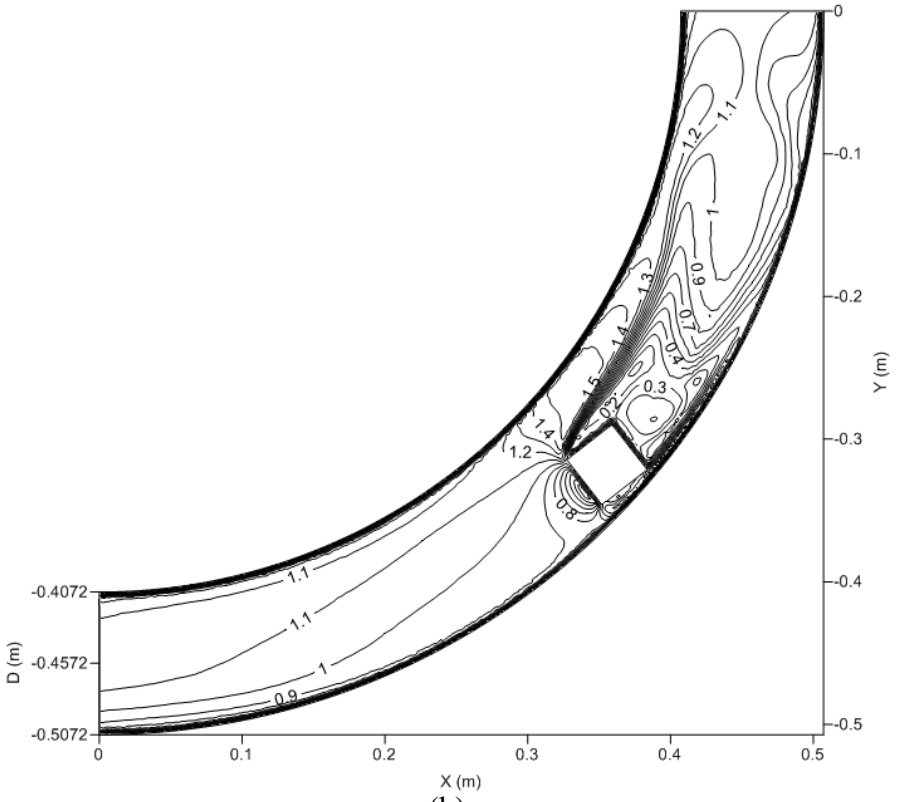
D (m)
-0.4072
-0.4572
-0.5072
X (m)
0
0.1
0.2
0.3
0.4
0.5
Y (m)
-0.1
-0.2
-0.3
-0.4
-0.5
1.1
1.2
1
0.9
1.3
1.4
1.5
0.7
0.6
0.3
0.2
0
0.8

(b)

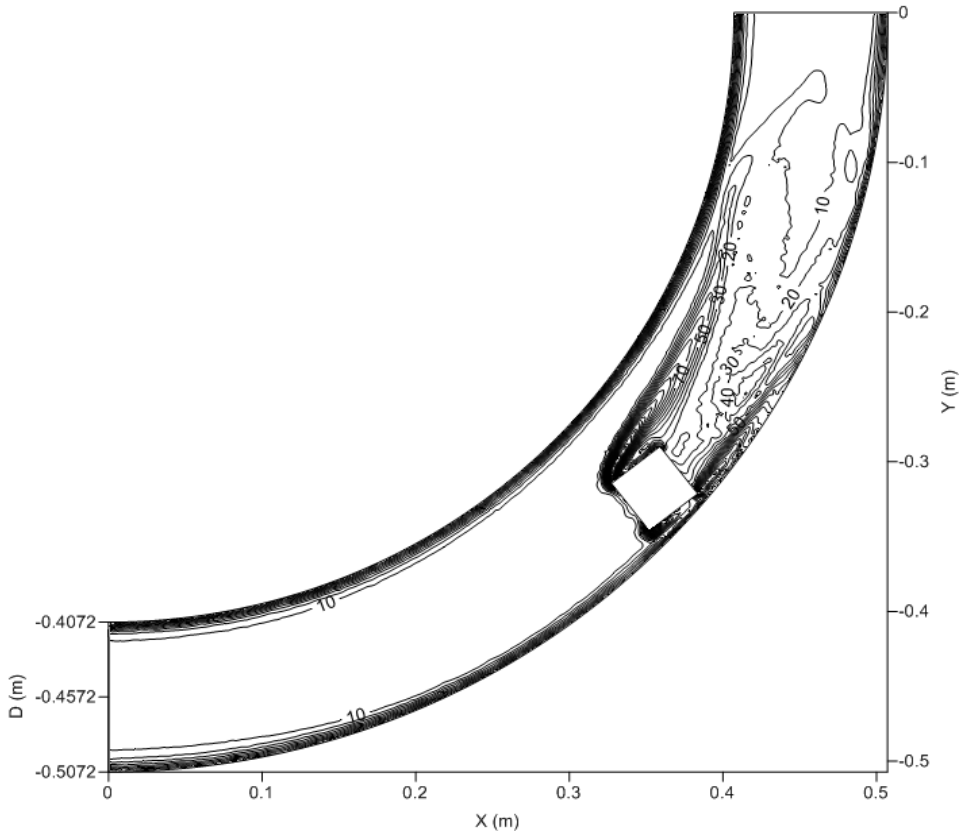

(c)

Figure 14 Flow fields within a horizontal 90º HCP bend of R/r=8, transporting a single equi-density rectangular capsule of k=0.4 and L_c=1d_h at U_{av}=1m/sec (a) Static pressure (Pa) (b) Velocity magnitude (m/sec) (c) Vorticity magnitude (/sec)

The pressure drop in this particular case is 345Pa(g), which is 21.1% less than for R/r=4, and 8.1% higher than the pressure drop within a horizontal pipeline carrying rectangular capsule of the same size. Ω_c has been computed to be 0.455 in the present case.

8.9 Capsule's Friction Factor Prediction Models

Mixture static gauge pressure variations and a novel parameter to quantify losses within HCPs transporting rectangular capsules have been discussed in detail in the previous section. There is a need to develop semi-empirical prediction models for capsule's friction factor and loss coefficient that can be used to design a hydraulic capsule pipeline. These prediction models have been developed using advanced statistical tools such as multiple variable regression analysis. The capsule's friction factors and loss coefficients have been expressed as a function of the different geometric and flow related variables considered in the present study. Table 6 summarises the developed prediction models for various cases.

Table 6 Friction factors and Loss coefficients of capsules in HCPs

Pipeline Orientation	Density of the Capsules	Pipe/Bend	λ_c and Ω_c Expressions
Horizontal	Equi-Density	Pipe	$\lambda_c = \frac{\left(14.8 \left(\frac{N}{Lp} * Lc\right)^{1.12} k^{2.5} \left(\frac{S+Lp}{Lp}\right)^{0.7}\right)}{Re_{pr}{}^{0.0427} \frac{Lc}{d}^{1.05}}$
		Bend	$\Omega_c = \frac{\left(4140 \left(\frac{N}{Lp} * Lc\right)^{2.31} k^{1.71} \left(\frac{S+Lp}{Lp}\right)^{1.39}\right)}{Re_{pr}{}^{0.024} \frac{R}{r}^{3.61} \frac{Lc}{d}^{2.43}}$
	Heavy-Density	Pipe	$\lambda_c = \frac{\left(58.8 \left(\frac{N}{Lp} * Lc\right)^{1.98} k^{1.76} \left(\frac{S+Lp}{Lp}\right)^{1.73}\right)}{Re_{pr}{}^{0.04} \frac{Lc}{d}^{1.93}}$
		Bend	$\Omega_c = \frac{\left(9120 \left(\frac{N}{Lp} * Lc\right)^{2.57} k^{1.54} \left(\frac{S+Lp}{Lp}\right)^{1.62}\right)}{Re_{pr}{}^{0.058} \frac{R}{r}^{0.48} \frac{Lc}{d}^{2.64}}$
Vertical	Equi-Density	Pipe	$\lambda_c = \frac{\left(52.48 \left(\frac{N}{Lp} * Lc\right)^{1.64} k^{2} \left(\frac{S+Lp}{Lp}\right)^{1.29}\right)}{Re_{pr}{}^{0.06} \frac{Lc}{d}^{1.55}}$
		Bend	$\Omega_c = \frac{\left(6309 \left(\frac{N}{Lp} * Lc\right)^{2.53} k^{1.41} \left(\frac{S+Lp}{Lp}\right)^{1.68}\right)}{Re_{pr}{}^{0.043} \frac{R}{r}^{0.48} \frac{Lc}{d}^{2.63}}$
	Heavy-Density	Pipe	$\lambda_c = \frac{\left(70.8 \left(\frac{N}{Lp} * Lc\right)^{1.69} k^{1.97} \left(\frac{S+Lp}{Lp}\right)^{1.36}\right)}{Re_{pr}{}^{0.079} \frac{Lc}{d}^{1.56}}$
		Bend	$\Omega_c = \frac{\left(2450 \left(\frac{N}{Lp} * Lc\right)^{2.05} k^{1.96} \left(\frac{S+Lp}{Lp}\right)^{1.08}\right)}{Re_{pr}{}^{0.0067} \frac{R}{r}^{0.55} \frac{Lc}{d}^{2.18}}$

Where Re_{pr} is the Reynolds number of the capsule/s, which can be calculated as:

$$Re_{pr} = \frac{\rho_c U_c d_h}{\mu} \tag{16}$$

All 576 numerical predictions regarding the pressure drop across the HCP have been used to develop the semi-empirical prediction models of table 6. For this purpose, advanced statistical tools like multiple variable regression has been employed. In order to check the validity of these prediction models, λ_c and Ω_c from these models have been compared against CFD predicted λ_c and Ω_c values. An example of comparison of λ_c is shown in figure 15 (for

equi-density rectangular capsules in a horizontal pipe). It can be seen that more than 90% of the data points lie within ±10% error band.

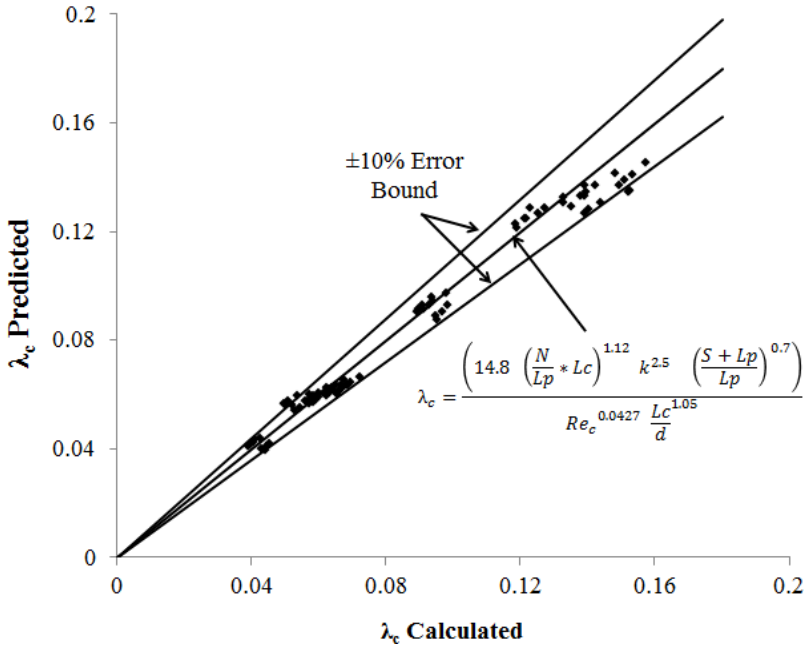

Figure 15 An example of comparison between computed and predicted capsule friction factors

9. Optimisation of HCPs

Optimisation of HCPs is vital for its commercial viability of transportation system. An optimisation model, based on Least-Cost Principle, has already been developed by the author in a previous study [26]. That optimisation model has been configured to work with the rectangular capsules in the present study. The model is based on the least-cost principle, i.e. the pipeline transporting capsules is designed such that the total cost of the pipeline is minimum. The total cost of a pipeline transporting capsules consists of the manufacturing cost of the pipeline and the capsules plus the operating cost of the system.

$$Cost_{Total} = Cost_{Manufacturing} + Cost_{Operating} \tag{17}$$

The manufacturing cost can be further divided into the cost of the pipeline and the cost of the capsules. The operating cost refers to the cost of the power being consumed.

$$Cost_{Total} = Cost_{Pipe} + Cost_{Capsule} + Cost_{Power} \tag{18}$$

9.1 Cost of Pipes

The cost of pipe per unit weight of the pipe material is given by [54]:

$$Cost_{Pipe} = \pi D t \gamma_p \chi_2 L_p \tag{19}$$

where t is the thickness of the pipe wall, γ_p is the specific weight of the pipe material and χ_2 is the cost of the pipe per unit weight of the piping material. According to Davis and Sorenson [55], and Russel [56], the pipe wall thickness can be expressed as:

$$t = \chi_c D \tag{20}$$

where χ_c is a constant of proportionality dependent on expected pressure and diameter ranges of the pipeline. Hence, the cost of the pipe becomes:

$$C_{ostPipe} = \pi D^2 \gamma_p \chi_2 \chi_c L_p \tag{21}$$

9.2 Cost of Capsules

The cost of rectangular capsules per unit weight of the capsule material can be calculated as:

$$Cost_{Rectangular\ Capsules} = \pi k D L_c t_c N \gamma_C \chi_3 \tag{22}$$

where t_c is the thickness of the capsule, N is the total number of capsules in the pipeline, Lc is the length of the capsule and γ_c is the specific weight of the capsule material.

9.3 Cost of Power

The cost of power consumption per unit watt is given by:

$$Cost_{Power} = \chi_1 P \tag{23}$$

Where P is the power requirement of the pipeline transporting capsules. It is the power that dictates the selection of the pumping unit to be installed. The power can be expressed as:

$$Power = \frac{Q_m \ \Delta P_{Total}}{\eta} \tag{24}$$

where Q_m is the flow rate of the mixture, ΔP_{Total} is the total pressure drop in the pipeline transporting capsules and η is the efficiency of the pumping unit. Generally the efficiency of industrial pumping unit ranges between 60 to 75%. The total pressure drop can be calculated from the friction factor (and loss-coefficient) models developed.

9.4 Mixture Flow Rate

Liu reports the expression to find the mixture flow rate for a circular pipe as [49]:

$$Q_m = \frac{\pi D^2}{4} U_{av} \tag{25}$$

9.5 Total Pressure Drop

The total pressure drop in a pipeline can be expressed as a sum of the major and minor pressure drop and minor pressure drop resulting from pipeline and pipe fittings respectively [35]. These pressure drops have already been defined in equation (5-9), were λ_w can be found by the Moody's approximation as [52]:

$$\lambda_w = 0.0055 + \frac{0.55}{Re_w^{\frac{1}{3}}} \tag{26}$$

and Ω_w has been found out to be:

$$\Omega_w = \frac{\left(3.05 - 0.0875\frac{R}{r}\right)}{Re_w^{\frac{1}{5}}} \quad (27)$$

9.6 Solid Throughput

The solid throughput, in m^3/sec, is the only input to the optimisation model developed here, which can be represented as:

$$Q_c = k^2 D^2 L_c \ \frac{N}{\mathrm{r}} \quad (28)$$

where r is the time taken by the capsule train to travel unit length. The length of the test section can be expressed as:

$$L_p = NL_c + (N-1)S \quad (29)$$

where N is the number of capsules and can be represented as:

$$N = \frac{L_p + S}{L_c + S} \quad (30)$$

Hence:

$$Q_c = \frac{k^2 D^2 L_c U_c}{L_p} \ x \ \frac{L_p + S}{L_c + S} \quad (31)$$

Hence, U_c can be represented in terms of Q_c. Furthermore, U_{av} can be expressed in terms of U_c from the DPM predictions ($U_{av} = 1.14U_c$). The following steps should be followed to run the optimisation model:

1. Assume a value of D
2. The length of the pipeline is already known from the information of the capsules injection and evacuations sites
3. Calculate the cost of pipes and capsules based on the information regarding the materials of the pipe and the capsules, and the market price of these materials (equations (21-22))
4. Fix the value of k
5. Assume the value of the efficiency of the pumping unit (0.6-0.75)
6. Calculate U_{av}, U_c, Re_w and Re_c (equations (31) and (16))
7. Calculate friction factors and pressure drop (both major and minor, equation (26-27), and (5-9))
8. Calculate Q_m (equation (25))
9. Find out the power requirement for the system (equation (24))

10. Calculate the total cost of the pipeline based on the cost of per unit of electricity (equation (21-23))

Repeat steps 1 to 10 for various values of D until that value is reached at which the total cost of the pipeline is minimum

10. Design Example

Equi-density rectangular capsules of k=0.5 need to be transferred from the processing plant to the storage area of the factory half kilometre away. The spacing between the capsules has been set at $3d_h$. The required throughput is 1kg/sec. Find the optimal size of the pipeline and the pumping power required for this purpose.

Solution: According to the current market, the values of χ_1, χ_2, χ_3, and χ_c are 1.4, 1.1, 0.95 and 0.01 respectively [26-28]. The pumping unit's efficiency is assumed to be 60%. It is noteworthy from the results obtained after following the aforementioned steps for optimisation that the manufacturing cost is a one-off cost, whereas the cost of power consumption is an annual cost.

The results presented in figure 16 depict as the diameter of the HCP increases the manufacturing cost also increases, whereas the cost of pumping power decreases. The decrease in the pumping cost is due to the decrease in the average flow velocity for a bigger diameter pipe. Furthermore, it can be clearly seen that the total cost of the pipeline first decreases from pipeline diameter of 80mm to 110mm, and then starts increasing as pipeline diameter further increases. Hence, the optimal pipeline diameter, corresponding to the minimum total cost, is 110mm. The power of the pumping unit required, corresponding to the optimal diameter of the pipeline, is 4.04kW. For the same required solid throughput and operational conditions (k, Lc, S etc.), the optimal pipeline diameter for cylindrical capsules is 90mm, where the corresponding pumping power required is 2.68kW.

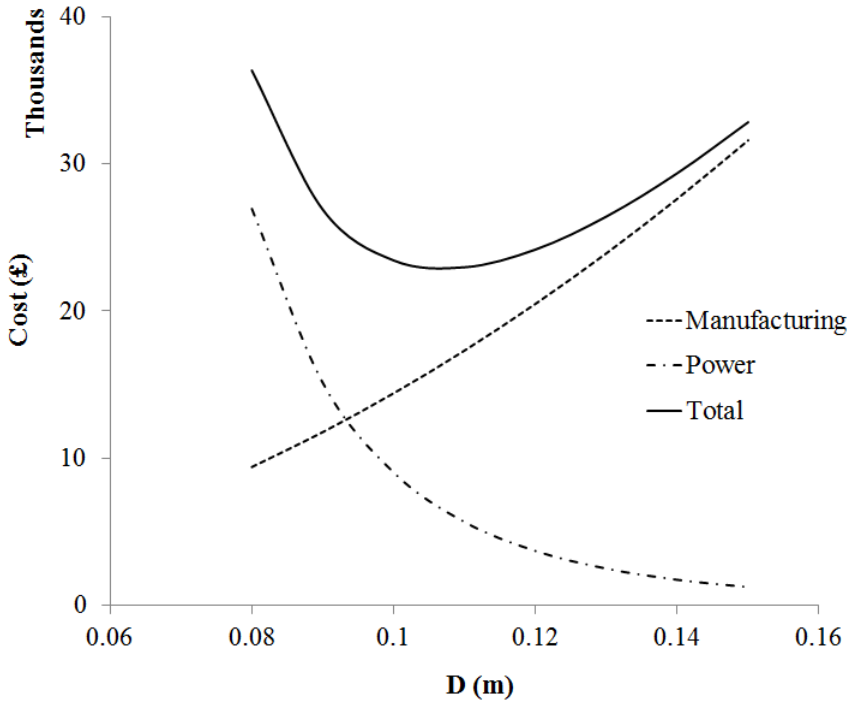

Figure 16 Variations in pipeline costs with the diameter

11. Conclusions

From the results presented in the present study, it can be concluded that the presence of rectangular capsule/s within a hydraulic pipeline alters the flow behaviour considerably and hence increases the pressure losses. Detailed analysis of the flow parameters' variations for different geometrical and flow configurations has revealed that the flow fields within an HCP vary significantly as the capsule concentration, size, density, flow velocity, pipe's inclination varies. Increase in capsule concentration and spacing increases the pressure drop within an HCP, while increasing the length of the capsule has marginal effects on the pressure drop. Furthermore, increase in capsule hydraulic diameter increases the pressure drop across the pipeline. Heavier rectangular capsules offer more resistance to the flow because of asymmetric and highly non-uniform flow behaviour within the HCPs, adding to the pressure losses. Similarly, increasing the average flow velocity increases the pressure drop across the pipeline; however the overall flow structure in the vicinity of the capsule remains the same.

It has also been observed that although the pressure drop across a vertical HCP is considerably higher as compared to a horizontal HCP, however, pressure loss contributions due to presence of the capsules in the flow field remain almost constant, and the primary contributing factor for pressure loss is the elevation of the pipeline. Moreover, it has been noticed that pressure drop across pipe bends is higher as compared to a straight pipeline, and increasing its R/r lowers the pressure drop across the pipe bend. Based on the pressure drop results, novel semi-empirical prediction models have been developed for the friction factor/s and loss coefficient/s of the capsule/s, which have been embedded into a pipeline optimisation model that is based on least-cost principle. The optimisation model's only input is the solid throughput required from the HCP, while the primary output is the optimal pipeline diameter. A practical example has been included in order to demonstrate the usage and effectiveness of this optimisation model.

NOMENCLATURE

c	Concentration of Solid Phase (%)
d_h	Hydraulic Diameter of the Capsule/s (m)
D	Diameter of Pipe (m)
g	Acceleration due to gravity (m/sec^2)
z	Elevation (m)
H	Holdup (-)
k	Capsule to Pipe diameter ratio (-)
L	Length (m)
n	Number of Bends (-)
N	Number of Capsules (-)
P	Local Static Pressure (Pa)
Q	Flow Rate (m^3/sec)
R	Radius of Curvature of Pipe Bend (m)
r	Radius of Pipe (m)
Re	Reynolds Number (-)
s	Specific Gravity (-)
S	Spacing between the Capsules (m)
t	Thickness (m)
U	Velocity (m/sec)
X	X direction
Y	Y direction

GREEK SYMBOLS

χ_c	Constant of Proportionality (-)
χ_1	Cost of Power consumption per unit Watt (£/W)
χ_2	Cost of Pipe per unit weight of pipe material (£/N)
χ_3	Cost of Capsules per unit weight of capsule's material (£/N)
λ	Darcy Friction Factor (-)
Ω	Loss Coefficient of Bends (-)
γ	Specific Weight (N/m^3)
Δ	Change
ε	Roughness Height of the Pipe (m)
η	Efficiency of the Pump (%)
θ	Angular Position (º)
μ	Dynamic Viscosity (Pa-sec)
л	Pi
ρ	Density (Kg/m^3)
Ψ	Shape factor (-)
r	Time (sec)

SUBSCRIPTS

av	Average
c	Capsule
con	Concentration
h	Hydraulic
m	Mixture
p	Pipe
pr	Particle
w	Water
∞	Free Stream

References

[1] M. E. Charles, Theoretical Analysis of the Concentric Flow of Cylindrical Forms, The Canadian Journal of Chemical Engineering, 41 (1962) 46–51.

[2] H. S. Ellis, An Experimental Investigation of the Transport by Water of Single Cylindrical and Spherical Capsules with Density Equal to that of the Water, The Canadian Journal of Chemical Engineering, 42 (1964) 1–8.

[3] R. Newton, P. J. Redberger, G. F. Round, Numerical Analysis of Some Variables Determining Free Flow, The Canadian Journal of Chemical Engineering, 42 (1963) 168–173.

[4] H. S. Ellis, An Experimental Investigation of the Transport in Water of Single Cylindrical Capsule with Density Greater than that of the Water, The Canadian Journal of Chemical Engineering, (1964) 69–76.

[5] J. Kruyer, P. J. Redberger, H. S. Ellis, The Pipeline Flow of Capsules, Part 9, Journal of Fluid Mechanics, 30 (1967) 513–531.

[6] Y. Tomita, M. Yamamoto, K. Funatsu, Motion of a Single Capsule in a Hydraulic Pipeline, Journal of Fluid Mechanics, 171 (1986) 495–508.

[7] Y. Tomita, T. Okubo, K. Funatsu, Y. Fujiwara, Unsteady Analysis of Hydraulic Capsule Transport in a Straight Horizontal Pipeline, In the Proceedings of the 6th International Symposium on Freight Pipelines, Eds. H. Liu and G. F. Round, USA, (1989) 273–278.

[8] C. W. Lenau, M. M. El-Bayya, Unsteady Flow in Hydraulic Capsule Pipeline, Journal of Engineering Mechanics, 122 (1996) 1168–1173.

[9] M. F. Khalil, S. Z. Kassab, I. G. Adam, M. A. Samaha, Turbulent Flow around a Single Concentric Long Capsule in a Pipe, Journal of Applied Mathematical Modelling, 34 (2010) 2000–2017.
[10] H. S. Ellis, Minimising the Pressure Gradients in Capsule Pipelines, The Canadian Journal of Chemical Engineering, 52 (1974) 457–462.
[11] J. Kruyer, W. T. Snyder, Relationship between Capsule Pulling Force and Pressure Gradient in a Pipe, The Canadian Journal of Chemical Engineering, 53 (1975) 378–383.
[12] H. H. Kroonenberg, A Mathematical Model for Concentric Horizontal Capsule Transport, The Canadian Journal of Chemical Engineering, 57 (1979) 383.
[13] V. C. Agarwal, R. Mishra, Optimal Design of a Multi-Stage Capsule Handling Multi-Phase Pipeline, International Journal of Pressure Vessels and Piping, 75 (1998) 27–35.
[14] K. W. Chow, An Experimental Study of the Hydrodynamic Transport of Spherical and Cylindrical Capsules in a Vertical Pipeline, M. Eng. Thesis, McMaster University, (1979), Hamilton, Ontario, Canada.
[15] L. Y. Hwang, D. J. Wood, D. T. Kao, Capsule Hoist System for Vertical Transport of Coal and Other Mineral Solids, The Canadian Journal of Chemical Engineering, 59 (1981) 317–324.
[16] B. Latto, K. W. Chow, Hydrodynamic Transport of Cylindrical Capsules in a Vertical Pipeline, The Canadian Journal of Chemical Engineering, 60 (1982) 713–722.
[17] M. Tachibana, Basic Studies on Hydraulic Capsule Transportation, Part 2, Balance and Start-up of Cylindrical Capsule in Rising Flow of Inclined Pipeline, Bulletin of the JSME, 26 (1983) 1735–1743.
[18] D. Ulusarslan, I. Teke, An Experimental Determination of Pressure Drops in the Flow of Low Density Spherical Capsule Train Inside Horizontal Pipes, Journal of Experimental Thermal and Fluid Science, 30 (2006) 233–241.
[19] D. Ulusarslan, Determination of the Loss Coefficient of Elbows in the Flow of Low-Density Spherical Capsule Train, Experimental Thermal and Fluid Science, 32 (2007) 415–422.
[20] D. Ulusarslan, I. Teke, Relation between the Friction Coefficient and Re Number for Spherical Capsule Train-Water Flow in Horizontal Pipes, Particulate Science and Technology, 27 (2009) 488–495.
[21] D. Uluasarslan, Comparison of Experimental Pressure Gradient and Experimental Relationships for the Low Density Spherical Capsule Train with Slurry Flow Relationships, Powder Technology, 185 (2008) 170–175.
[22] I. Teke, D. Uluasarslan, Mathematical Expression of Pressure Gradient in the Flow of Spherical Capsules Less Dense than Water, International Journal of Multiphase Flow, 33 (2007) 658–674.
[23] P. Vlasak, J. Myska, The Effect of Pipe Curvature on the Flow of Carrier Liquid Capsule Train System, In the Proceedings of the Institute of Hydrodynamics, (1983) Praha.
[24] P. Vlasak, V. Berman, A Contribution to Hydro-transport of Capsules in Bend and Inclined Pipeline Sections, Handbook of Conveying and Handling of Particulate Solids, (2001) 521–529.
[25] R. Mishra, S. N. Singh, V. Seshadri, Improved model for the prediction of pressure drop and velocity field in multi-sized particulate slurry flow through horizontal pipes, Powder Handling and Processing, 10 (1998) 279–287.
[26] T. Asim, Computational Fluid Dynamics based Diagnostics and Optimal Design of Hydraulic Capsule Pipelines, Ph.D. Thesis, University of Huddersfield, (2013), Huddersfield, U.K.
[27] T. Asim, R. Mishra, Optimal Design of Hydraulic Capsule Pipeline Transporting Spherical Capsules, The Canadian Journal of Chemical Engineering, In Press, (2015).

[28] T. Asim, R. Mishra, Computational Fluid Dynamics Based Optimal Design of Hydraulic Capsule Pipelines Transporting Cylindrical Capsules, Powder Technology, In Press, (2016).
[29] H. G. Polderman, Design Rules for Hydraulic Capsule Transport Systems, Journal of Pipelines, 3 (1982) 123–136.
[30] M. Assadollahbaik, H. Liu, Optimum Design of Electromagnetic Pump for Capsule Pipelines, Journal of Pipelines, 5 (1986) 157–169.
[31] Y. Sha, X. Zhao, Optimisation Design of the Hydraulic Pipeline Based on the Principle of Saving Energy Resources, In the Proceedings of Power and Energy Engineering Conference, (2010) Asia-Pacific.
[32] P. K. Swamee, Design of Sediment Transporting Pipeline, Journal of Hydraulic Engineering, 121 (1995).
[33] Swamee, Prabhata. K, Capsule Hoist System for Vertical Transport of Minerals, Journal of Transportation Engineering, (1999) 560–563.
[34] H. Darcy, Recherches Expérimentales Relatives au Mouvement de l'Eau dans les Tuyaux [Experimental Research on the Movement of Water in Pipes], Mallet-Bachelier (1857) Paris.
[35] B. R. Munson, D. F. Young, T. H. Okiishi, Fundamentals of Fluid Mechanics, John Willey & Sons Inc., 4th ed., (2002) U.S.A.
[36] D. Ulusarslan, I. Teke, An Experimental Investigation of the Capsule Velocity, Concentration Rate and the Spacing between the Capsules for the Spherical Capsule Train Flow in a Horizontal Circular Pipe, Powder Technology, 159 (2005) 27–34.
[37] Industrial Accessories Company accessible at http://www.iac-intl.com/parts/PB103001r2.pdf
[38] R. Mishra, E. Palmer, J. Fieldhouse, An Optimization Study of a Multiple-Row Pin-Vented Brake Disc to Promote Brake Cooling Using Computational Fluid Dynamics, Proceedings of the Institution of Mechanical Engineers, Part D: Journal of Automobile Engineering, 223 (2009) 865–875.
[39] R. Mishra, S. N. Singh, V. Seshadri, Velocity measurement in solid-liquid flows using an impact probe, Flow Measurement and Instrumentation, 8 (1998) 157–165.
[40] S. A. Morsi, A. J. Alexander, An Investigation of Particle Trajectories in Two-Phase Flow Systems, Journal of Fluid Mechanics, 55 (1972) 193–208.
[41] H. A. Stone, Philip Saffman and Viscous Flow Theory, Journal of Fluid Mechanics, 409 (2000) 16–183.
[42]
[43] D. Ulusarslan, Effect of Capsule Density and Concentration on Pressure Drops of Spherical Capsule Train Conveyed by Water, Journal of Fluids Engineering, 132 (2009).
[44] C. Ariyaratne, Design and Optimisation of Swirl Pipes and Transition Geometries for Slurry Transport, Ph.D. Thesis, (2005), The University of Nottingham.
[45] M. Rosenfeld, E. Rambod, M. Gharib, Circulation and Formation Number of Laminar Vortex Rings, Journal of Fluid Mechanics, 376 (1998) 297–318.
[46] K. Mohseni, M. Gharib, A Model for Universal Time Scale of Vortex Ring Formation, Physics of Fluids, 10 (1998) 2436–2438.
[47] M. Gharib, E. Rambod, K. Shariff, A Universal Time Scale for Vortex Ring Formation, Journal of Fluid Mechanics, 360 (1998) 121–140.
[48] M. Shusser, M. Gharib, Energy and Velocity of a Forming Vortex Ring, Physics of Fluids, 12 (2002) 618–621.
[49] H. Liu, Pipeline Engineering, CRC Press, (2003) U.S.A.
[50] J. Feng, P. Y. Huang, D. D. Joseph, Dynamic Simulation of the Motion of Capsules in Pipelines, Journal of Fluid Mechanics, 286 (1995) 201–227.

[51] K. Yanaida, M. Tanaka, Drag Coefficient of a Capsule Inside a Vertical Angular Pipe, Powder Technology, 94 (1997) 239–243.
[52] L. F. Moody, Friction Factors for Pipe Flow, Transactions of the ASME, 66 (1944) 671–684.
[53] R. Mishra, S. N. Singh, V. Seshedri, Study of Wear Characteristics and Solid Distribution in Constant Area and Erosion-Resistant Long-Radius Pipe Bends for the flow of Multisized Particulate Slurries, Wear, 217 (1998) 297–306.
[54] P. N. Cheremisinoff, S. I. Cheng, Civil Engineering Practice, Technomies Publishing Co., (1988) U.S.A.
[55] C. Davis, K. Sorensen, Handbook of Applied Hydraulics, McGraw-Hill Book Co., 3rd ed., (1969) U.S.A.
[56] G. Russel, Hydraulics, Holt, Rinehart and Winston, 5th ed., (1963) U.S.A.